Development of peptides for use as antimicrobial agents

by

Ali Shukri

A thesis submitted to the Faculty of Graduate and Postdoctoral Affairs in partial fulfillment of the requirements for the degree of

Master of Science

in

Biology

Carleton University
Ottawa, Ontario

Abstract

Pathogenic bacteria are evolving resistance to conventional therapeutics at a rate which threatens our ability to reliably treat common infections, necessitating the discovery of new therapeutics. In this thesis, I look at the development of novel peptides that can be used to combat antimicrobial resistance. In Chapter 2, I employ a permutation of two known antimicrobial peptides (AMPs), Indolicidin and UyCT3, and through sequential generations of evolution, develop a peptide that can inhibit bacterial growth better than the wild type AMP. These AMPs are tested on clinically derived strains to help translate the clinical relevance of these findings. In Chapter 3, I use an orientated peptide array library (OPAL) to assist in the discovery of peptide β-lactamase inhibitors against the β-lactamase TEM-1. Candidates' activities were assessed for inhibition against TEM-1. These results show the significance of our findings and the robustness of the techniques that can be used for the discovery of peptide antimicrobials.

Acknowledgements

I would first like to express my most sincere gratitude to both of my supervisors, Dr. Kyle Biggar, and Dr. Alex Wong. I knew being co-supervised would be a challenge but having both of you as my supervisors was an honour. To Alex: thank you for accepting me into your lab and taking me on as a co-supervised student. You were always very patient and helpful throughout the whole process. Your knowledge, sincerity, and compassion are attributes that make you a great mentor. To Kyle: I am deep indebted to you for first taking me on a student in 2019. Who knew that you would take me on a graduate student a few months later? You were always available for questions and compassionate along the way.

I would like to express my gratitude towards my committee members, Dr. Sue Twine and Dr. Christopher Boddy, for their supportive discussions and engouements through the process of this graduate degree.

Being co-supervised allowed me to be part of two amazing labs. For my friends in the Wong lab, I would like to thank you for all the laughs, tips, and tricks, and all the guidance you have provided for me. I want to also say thank you for letting me use the plate reader for days at a time to run my growth curves. I would also like to personally thank Dr. Amanda Carroll who helped me in the first few weeks as I transitioned into the lab environment. Thank you to Dr. Aaron Hinz for all your help with the integra robot and to bounce ideas off each other. Thank you, Caitlin, for talking about books whenever we both found the time to read in grad school. Thank you to Asalia for all the jokes along the way. Thank you Amer for always having a caring smile.

For my friends in the Biggar lab, thank you for making all the time spent in the lab even more fun. Thank you to Dr. Valentina Lukinovic, who always ensured our lab ran smoothly and for becoming one of my close friends. Thank you to Matt Hoekstra for always cracking jokes and being there for when stuff went wrong (which was a lot). Thank you to Anand for all your help, guidance, and knowledge on Biochemistry.

I would love to give my highest gratitude to Dr. Taylor Alison Swift for her musical discography, for her music pushed me through this degree.

Finally, I would like to thank my family and friends for constantly asking me what my research is about, me explaining it, and them asking me about it again a week later.

Statement of contribution

Chapter 2, 'Systematic *in vitro* optimization of antimicrobial peptides against *Escherichia coli*', is a result of experiments that were primarily designed by me, Dr. Amanda Carroll, Ryan Collins, Dr. Alex Wong, and Dr. Kyle Biggar. This was written by me with contributions from Dr. Alex Wong. The initial peptide library was synthesized by Ryan Collins, and testing was performed by Dr. Amanda Carroll. Peptide clustering's was performed by Francois Charih. I performed the data analysis of the 1st generation, synthesis of 2nd peptide generation, and growth curve acquisition and analysis for both MG1655 and the three clinical strains.

Chapter 3, 'Development of peptide based β-lactamase inhibitors against TEM-1 using an Orientated Peptide Array Library and evaluating inhibition using nitrocefin', is a result of experiments that were designed and carried out by me with contributions from Dr. Kyle Biggar. Peptide clustering was performed by Francois Charih.

Table of Contents

List of Tables

 # Title Page

List of Illustrations

 # Title Page

List of Appendices

Chapter 1:

Introduction to Antimicrobial Resistance

1.1 General introduction

Since their discovery, antibiotics have been administered and have saved innumerable lives around the world (Hasan *et al*., 2022). However, antibiotics are now proving to be less effective than they were when first discovered (Golkar *et al*., 2014; Iskander *et al*., 2022). Pathogens are starting to evolve resistance to conventional antibiotics at a rate which threatens our ability to combat it. Antimicrobial resistance (AMR) poses an extreme risk to public health, for both developing and developed nations (Llor and Bjerrum, 2014; Ventola, 2015). AMR is defined as the ability for bacterium, fungi, and/or parasites to survive in a drug environment that previously impacted them. These resistant bacteria are often referred to as 'superbugs', and they are emerging as global threats (Dadgostar, 2019). The prevalence of these cases, as well as increases over a 4-year gap, show the rising issue of AMR. This information highlights the dire consequences that AMR has down the line, and if immediate action is not taken, there will be even more unfavourable outcomes (PHAC, 2020).

Although different actions are being taken, the prevalence of resistant pathogens is increasing yearly with no plateau in sight, and thousands of lives are expected to be lost (Dadgostar, 2019). In 2018, 5,400 lives were lost as a direct result of AMR in Canada, with this number estimated to increase to 13,700 by the year 2050. AMR does not simply pose a health risk, but also a burden on the health-care system (projected $7.6 billion/year in 2050) and a socio-economic impact as well (reduction in Canadian GDP by $21 Billion annually) (PHAC, 2020). In the Canadian Antimicrobial Resistance Surveillance System report, there was a

nine-fold increase in patients harbouring carbapenem-resistant organisms between 2014 and 2018. There was also an increase in both prescription rates as well as antimicrobial purchasing by hospitals. It was also shown that 26% of infections in Canada are resistant to the first line of drugs that were used to treat them (PHAC, 2020). These statistics show the prevalence of AMR in the community and that necessary steps are needed to be taken.

1.2 Drivers of antimicrobial resistance

Sir Alexander Fleming had warned the world about the misuse of antibiotics and the susceptibility of bacteria to resistance against antibiotics more than 70 years ago (Fleming, 1945). Indeed, there are multiple factors that lead to the driving force of progressing AMR. It is shown that the overuse of antibiotics is a heavy factor that is driving the evolution of resistant bacteria (Read and Woods, 2014; Ventola, 2015), as well as the use of antibiotics in agriculture (Ventola, 2015).

Both overuse and misuse of antibiotics are a driving force for the emergence of resistant bacteria. In some countries, antibiotics are not as regulated as other drugs and can be purchased over the counter without any prescriptions. Even in countries where a prescription is needed, antibiotics are typically heavily over-prescribed (Michael *et al*., 2014; Nature, 2013). While overuse is a growing concern, there is also the issue of incorrectly prescribing antibiotics as a physician. It is estimated that half the antibiotics that are prescribed for acute respiratory tract infections are inappropriate and provide no benefit, other than its contribution to AMR development (Milani *et al*., 2019). Overuse of antibiotics also exposes

patients to the risk of increase adverse drug effects, where 24% of patients admitted with adverse drug side effects were due to antibiotics prescriptions (Milani *et al*., 2019). The emergence of these resistant pathogens is highly correlated to both the incorrect and inappropriate use of antibiotics (Luyt *et al*., 2014). There needs to be more regulatory measures put on the purchasing and distribution of antibiotics in healthcare settings.

Moving from an urban environment to rural, there are increased uses of antibiotics in various forms of live stocking and farming (Ventola, 2015). Over 80% of all antibiotics sold in Canada are administered to farm animals (Van Gerwen, 2017). Antibiotics are mainly being used as growth supplements in animal feed as a way of increasing the overall health of the animals, thus increasing the quality of the goods (Ventola, 2015). The transference of resistant bacteria was first documented over 40 years ago, when the gut flora of the farm animals and farmers were documented as being similar in composition (Bartlett *et al*., 2013; Ventola, 2015). Up to 90% of antibiotics that are used in agriculture are excreted through urine and stool, and are spread as manure, or into the ground water. Both excretions of antibiotics and resistant microorganisms by animals are a driving force. This leads to AMR being spread through the environment (Iwu *et al*., 2020). Various microbes have been found in humans that originated from animals, specifically methicillin resistant *Staphylococcus* strains as well as *Salmonella* (Chang *et al*., 2014).

1.3 Antibiotic mechanisms of action

Antibiotics are a diverse class of drugs that are known to have either bactericidal and/or bacteriostatic effects against bacterial and fungi infections (Reygaert, 2018). Antibiotics can be classified into different groups based on their mode of inhibition or based on structure. They can inhibit different cell processes such as DNA, protein, or cell wall synthesis (Reygaert, 2018). Shown in Table 1.1 are mechanisms of inhibition as well as classes of antibiotics. This is not an exhaustive list, but rather a summary. For example, antimicrobial peptides (AMPs) are a diverse class of antimicrobial agent that has varying effects on bacterial growth inhibition and can be characterized into one or more of the mechanisms of action shown in Table 1.1.

A major class of antibiotics is the β-lactams, which are named for their unique 4-membered ring structure which inhibits cell wall synthesis. The primary target of these antibiotics is Penicillin Binding Proteins (PBPs). Bacterial cells contain a cell wall that is made of peptidoglycan, a long sugar polymer. Neighboring peptidylglycan chains are crosslinked through their peptide side chains with the use of PBPs (Kapoor *et al*., 2017). These antibiotics and their mechanisms of resistance will be talked about in greater detail in chapter 3.

Another class of antibiotics are quinolones, which inhibit DNA synthesis. Quinolones interact with DNA machinery, specifically DNA gyrase and topoisomerase IV. Structurally, they take on a bicyclic ring form with fluorination of the compound showing increased antimicrobial activity (Kapoor *et al*., 2017).

Table 1.1 – Mechanisms of action and antimicrobial groups against gram-negative and gram-positive bacteria. Adapted from Reygaert, 2018.

Mechanism of Action	Antimicrobial Groups
Cell wall synthesis inhibition	β-lactams
	Carbapenems
	Cephalosporins
	Monobactams
	Penicillin
	Glycopeptides
Depolarize Cell Membrane	Lipopeptides
Protein synthesis inhibition	Binds to 30S Ribosomal unit
	Aminoglycosides
	Tetracyclines
	Binds to 50S Ribosomal unit
	Chloramphenicol
	Lincosamides
	Macrolides
	Oxazolidinones
	Streptogramins
Nucleic acid inhibition	Quinolones
	Fluoroquinolones
Metabolic pathways inhibitions	Sulfonamides
	Trimethoprim

1.4 Mechanisms of resistance

AMR occurs through a plethora of mechanisms. Resistance to antibiotics in bacteria can be caused by several biochemical pathways (Munita and Arias, 2016). There are four main categories that antibiotic resistance can fall into: limiting uptake of a drug, modifying a drug target, inactivating a drug, and active drug efflux (Reygaert, 2018).

Firstly, the uptake of antibiotics across the cellular membrane of bacteria is a mechanism of resistance that most bacteria employ. Drugs often enter the bacterial cells using porin channels. In gram negative bacteria, porin channels allow for hydrophilic drugs to cross the membrane. This drug uptake can be limited by one of two ways: mutations that change the selectivity of the porin channel, and a decrease in the number of porin channels that are expressed (Reygaert, 2018). The *Enterobacteriaceae* family are known to become resistance to carbapenems via a lowering in the expression of porin proteins. Bacterium such as *Klebsiella aerogenes* are resistant to imipenem and certain cephalosporins, while *Neisseria gonorrhoeae* has conferred resistance to β-lactams and tetracycline (Reygaert, 2018).

Another mechanism of resistance is the modification of a drug target. There are targets of antimicrobial agents within the bacterial cell, and many of these targets can be modified to allow for resistance to medication. A well-known mechanism of resistance to β-lactams is changes in the structure or number of PBPs (Reygaert, 2018). As stated previously, PBPs are important enzymes that are used in the construction of the peptidoglycan layer used in cell wall synthesis.

PBPs can have either mutations that do not allow binding to β-lactams, or limited expression of PBPs in the cell (Reygaert, 2018). An additional example of modifying drug targets is resistance to quinolone antibiotics. Quinolones interact with DNA gyrase and topoisomerase IV in both gram negative and gram-positive bacteria (Reygaert, 2018). However, quinolones primary target DNA gyrase in gram negative, while topoisomerase IV in gram positive bacteria. These proteins play key roles in supercoiling and uncoiling of DNA during replication, transcription, and recombination. Mutations in DNA gyrase A (*gyrA*) are known to be tied to quinolone resistance, specifically in the quinolone resistance determining region (QRDR) (Jaktaji and Mohiti, 2010). Other modifications of drug targets include 30S or 50S subunits used in protein translation, and binding of antibiotics such as vancomycin to D-alanyl-D-alanine residues in peptidoglycan precursors (Kapoor *et al*., 2017).

Another mechanism is the inactivation of drugs, whether it be through actual degradation of the drug, or by the transferance of a chemical group (Reygaert, 2018). Hydrolysis of β-lactams by β-lactamase enzymes across their amide bond is a prime example of this mechanism. Drug modification, as opposed to degradation, can involve transference of acetyl, phosphoryl, and adenyl groups (Kapoor *et al*., 2017). Examples of these chemical transferring groups include the inactivation of aminoglycosides by aminoglycoside modifying enzymes, as well as chloramphenicol acetyl transferases in most gram-positive and gram-negative bacteria (Kapoor *et al*., 2017).

Bacteria can also gain resistance by the removal of antibiotics from the intracellular space using drug efflux pumps (Reygaert, 2018). Efflux pumps are dynamic protein structures that regulate the outtake of antimicrobial agents. They can be either expressed constitutively or are induced or overexpressed under specific environments. Their primary role in bacterial cells is to remove toxic substances (Reygaert, 2018). Efflux pumps are diverse in their action, in particular which agents they pump out of the cell. Some efflux pumps can pump more than one type of substance, and they are referred to as multi drug efflux pumps (MDR efflux pump) (Reygaert, 2018). This specific mechanism can work by the expense of an ATP molecule, or even the exchange of ions (H^+ or Na^+). The understanding of how AMR is acquired through resistance pathways is important to forging the path to drug discovery (Munita and Arias, 2016).

1.5 Antibiotic drug discovery

Nearly one half of antibiotics used today originated from the ‘golden age’ of antibiotic research in the 1950s and 1960s. Since then, the AMR drug discovery pipeline has ‘dried up’. There have only been two new classes of antibiotics that have been brought forth for clinical use in the last two decades; oxazolidinone and cyclic lipopeptides (Coates *et al*., 2011). The development of new antibiotics is dampened by economic, regulatory, and scientific challenges (Bartlett *et al.,* 2013; Gould and Bal, 2013; Ventola, 2015).

The discovery of new antibiotics is very challenging (Lewis, 2020). Most antibiotics that are in use today were derived from natural sources, such as bacteria or plants (Nothias *et al*., 2016). Once this pool was exhausted, analogs of

known antibiotics were synthesized, and their antibacterial activity was assessed. For example, ampicillin and cephalosporins are derivatives of penicillin, and azithromycin is modified from erythromycin. Chemical group substitution has been utilized for different applications to enhance drug potency and allow for the discovery of new drugs from known drug candidates (Wright *et al*., 2014). However, resistance to derivatized versions of known drugs can evolve quickly through existing mechanisms of resistance against the origin antibiotic (Lewis, 2020; Tooke *et al*., 2019). Thus, there is an urgent need to develop novel therapeutics, including new drugs that inhibit bacterial growth, and those that inhibit resistance pathways towards known antibiotics.

Therapeutic peptides are a unique class of pharmaceutical agents that allow for a wide array of characteristics due to their unique make up. Therapeutic peptides can be dynamic in nature, ranging from small to large molecular weights (500-5000 Daltons) and structurally (helical, cyclic, etc) (Wang *et al*., 2022). Peptides can be used for a broad range of targets, towards which they can have high potency and selectivity (Recio *et al*., 2016; Vagner *et al*., 2008). Since the discovery and development of the first biotherapeutic peptide, insulin, in the 1920's, there has been tremendous development in the realm of peptide design, leading to the approval of over 80 peptides worldwide. Peptide drugs accounted for over $70 billion of the pharmaceutical market in 2019, which is a two-fold increase compared to 2013 (Wang *et al*., 2022).

Antimicrobial peptides (AMPs) are gaining traction as a new class of antimicrobials. They have substantial clinical potential due to their dynamic

chemical diversity and tertiary structure (Browne *et al*., 2020; Huan *et al*., 2020). AMPs are typically less than 100 amino acids in length, with positively charged and hydrophobic amino acids in their makeup. Due to their structure, they typically interact with cellular membranes directly, as opposed to the intracellular targets that small molecule antibiotics interact with (Browne *et al*., 2020). Naturally occurring AMPs have been documented across the tree of life, for example mammals, amphibians, and insects (Huan *et al*., 2020). Examples of AMPs include α and β-defensins, LL-37, colistin, Indolicidin, and UyCT3. It should be noted that this is not an exhaustive list, and that new AMPs are discovered yearly (Huan *et al.,* 2020; Luna-Ramirez *et al*., 2014; Mahlapuu *et al*., 2016).

In this thesis, I aim to investigate the use of peptides as therapeutics against antimicrobial resistance. This will be done through two main approaches:

1. Development of antimicrobial peptides with the use of a permutation screen of two known AMPs, Indolicidin and UyCT3. These peptides will go through subsequent generations of peptide evolution and their efficacy will be challenged against clinical strains. **My hypothesis is that permutations of amino acid residues in Indolicidin and UyCT3 will be able to increase the in antimicrobial activity beyond the WT peptide.**
2. Development of peptide β-lactamase inhibitors against rTEM-1 using degenerate orientated peptide array library (OPAL). Peptides will be tested for TEM-1 inhibition with nitrocefin as the substrate. **My hypothesis is that using peptide binding arrays, select interacting peptides will be able to disrupt the activity of the β-lactamase, TEM-1.**

Chapter 2:

Systematic *in vitro* optimization of antimicrobial peptides against *Escherichia coli*

Ali Shukri[1,2], Amanda Carroll[1,2], Ryan Collins[1,2], Francois Charih[1]

[1]Institute of Biochemistry, Carleton University, Ottawa Ontario, Canada K2J 0L6

[2]Department of Biology, Carleton University, Ottawa Ontario, Canada K2J 0L6

The rise of antibiotic resistant bacteria is a serious global health issue, with an estimated cost of $20 billion in medical expenses in the US in 2021. According to the Centre for Disease control (CDC), more than 2 million people are estimated to get ill with an antibiotic resistance infection, with approximately 23,000 lives taken per year (Dadgostar, 2019). Antimicrobial resistance (AMR) is defined as the ability for a microorganism to survive clinical doses of antibiotics that were previously sufficient to cure an infection. New antibiotic development is an important component of the fight against AMR, but is scientifically challenging, time consuming, and with little economic payoff. As such, the pace of new drug development has diminished since the 1980s, with fewer antimicrobial agents undergoing clinical trials (Chen and Lu, 2020; Dijksteel *et al.,* 2021). As such, there is a desperate need for new biomolecules targeting pathogenic bacteria.

Antimicrobial Peptides (AMPs) are a promising source of new antimicrobials (Bahar & Ren 2013). AMPs are usually small and positively charged peptides, composed of less than 100 amino acids with activity against fungi, yeast, viruses, and/or bacteria. Bactericidal activity is thought to derive from both the cationic and hydrophobic nature of some AMPs (Dijksteel *et al.,* 2021). These positively charged peptides will generally act against negatively charged bacterial cells, rather than the more neutral mammalian cells. Such AMPs integrate with and disrupt bacterial cell membranes, leading to cell death. In addition to antimicrobial activity, some AMPs are also known to participate in pathways which modulate the immune response (Dijksteel *et al.,* 2021).

Since their first discovery around the same time as penicillin in 1928, AMPs have been increasingly discussed in the literature and subjected to clinical trials as key antimicrobial agents. The first FDA approved AMP was nisin, a peptide used primarily as a food preservative. However, wide use of AMPs as antimicrobials has been limited by their toxicity to host cells, as well as other drawbacks such as manufacturing costs and time for synthesis (Dijksteel *et al.,* 2021).

Despite these challenges in translating *in vivo* antimicrobial effects into prescribable therapeutics, there are currently several AMPs undergoing clinical trials (Mahlapuu *et al.,* 2016, Strempel *et al.,* 2015). As of 2021, numerous AMPs are FDA approved, or undergoing human clinical trials (Dijksteel *et al.,* 2021), so there is a rise in the interest of AMPs as biotherapeutics. There are 7 AMPs that have had FDA approval: Gramicidin, Daptomycin, Colistin, Vancomycin, Ortivancin, Dalbavancin, and Telavancin. Numerous AMPs are currently in clinical trials, which shows the importance of the emergence of these biomolecules as antimicrobials (Dijksteel *et al.,* 2021).

AMPs currently used in the clinic were derived from natural sources, like colistin (polymyxin E) which is produced by the soil bacterium *Bacillus polymyxa* (El-Sayed Ahmed *et al*., 2020). The isolation, discovery, and characterization of AMPs through natural sources (serum, large databases, etc.) can be labour intensive and costly.

As a model for a new strategy for AMP development, I used systematic *in vitro* evolution to improve the activity of two known AMPs, Indolicidin and UyCT3, against the opportunistic pathogen *Escherichia coli*. Amino acid permutation and

subsequent peptide design can be used to optimize a known peptide sequence, potentially leading to the discovery of differences in structural integrity as well as peptide activity. This process involves point permutations of amino acids within defined peptide sequences to observe what changes in amino acids may elicit. This technique has been used in multiple biological applications, from identifying new substrates of lysine demethylases to the development of AMPs (Chopra *et al*., 2022; Hoesktra and Biggar, 2021; Mishra, *et al.,* 2020).

Indolicidin is a tridecapeptide (ILPWKWPWWPWRR) that was isolated from the cytoplasmic granules of bovine neutrophils (Subbalakshmi and Sitaram, 2006). It has broad and potent antimicrobial activity against both gram-negative and gram-positive bacteria. It is thought to bind abasic sites of DNA and interfere with the recruitment of DNA machinery, cause DNA filamentation, and to interact with DNA topoisomerase I (Hsu *et al.,* 2005; Huan *et al.,* 2020; Marchand *et al*., 2006). In addition, indolicidin may inhibit bacterial proteases (Huan *et al.,* 2020). This peptide is unusual in that it does not take on the typical alpha helical or β structure of other cationic peptides. With its high percentage of Tryptophan (Trp) residues, it adopts a wedge conformation with its hydrophobicity in the bacterial membrane. While indolicidin has substantial therapeutic potential, it has high toxicity towards mammalian cells (Nan *et al.,* 2009) with its toxicity toward red blood cells, yielding a high hemolytic activity.

UyCT3 is an alpha helical peptide derived from venom of the scorpion *Urodacus yaschenkoi* (Luna-Rameriz *et al.,* 2013). The full-length protein is 68 amino acids in length, but the sequence ILSAIWSGIKSLF is known to confer its

antimicrobial activity. It is a member of the non-disulfide-bridged peptide family (NDBP) as well as the small antimicrobial peptide group (Almaaytah and Albalas, 2014). UyCT3s mechanism of action is debated in the literature but is proposed to create a helical channel in the membrane of the bacterium, causing autolysis and ultimately bacterial death (Almaaytah and Albalas, 2014).

Through these techniques, I hope to optimize the antimicrobial profiles of these two AMPs and look at the applications of these methods for the development of future AMPs. Growth rates of the AMPs and their analogs was investigated in both WT MG1655 K-12, as well as three clinically relevant *E. coli* strains. The hemolytic activity of the best acting AMPs was assessed against sheep red blood cells to investigate toxicity to mammalian membranes.

2.2 Materials and Methods

2.2.1 Strains

The standard laboratory *E. coli* strain K-12 (MG1655) was used for screening of peptide libraries. Selected AMPs were tested against the clinically derived *E. coli* strains pb3, pb15, and pb35 that were provided from the Zhanel Laboratory from the University of Manitoba (Basra *et al.*, 2018). Their AMR profiles are shown in Table 2.1. A broad range of infections were chosen as to examine the ability of our peptides to inhibit growth of different pathogens. All strains were grown in Mueller Hinton Broth (MHB) purchased from Sigma Aldrich.

2.2.2 Peptide Synthesis

For the creation of our AMP peptide library, we systematically mutated each residue in both Indolicidin and UyCT3. Each residue was mutated to one of the remaining 19 amino acids, while keeping the rest of the AMP sequence constant. This led to the synthesis of 520 unique peptides, 260 each for Indolicidin and UyCT3.

Peptides were synthesized using Solid Phase Fmoc (N-(9-fluorenyl) methoxycarbonyl) chemistry using a ResPep SL peptide synthesizer (Intavis) at a 2 μmol scale using Rink-NH_2 resin. All amino acid derivates and activator were purchased from p3bio systems. To allow for quantification, peptides were synthesized with a C-terminal tryptophan separated from the peptide by a 6-aminohecanoic acid (6-ahx) linker. After synthesis, peptides were released from the resin and protecting groups were cleaved using an acidic cleavage solution (95 % trifluoroacetic acid, 3 % tri-isopropylsilane, 2 % water). Cold di-ethyl ether (-20 °C) was used to precipitate and wash the peptides of residual cleavage solution. Once dried, pellets were dissolved in 1X PBS containing 4% acetic acid. Peptides were brought up to pH 7 using 5 M NaOH and quantified by A280 and molar extinction coefficients calculated by ProtParam Expasy.

Table 2.1. **Tabulated information on clinical strains.** Cip = ciproflaxin, Cef = cefatazidime. Bolded mutations refer to mutations that lead to resistance phenotype.

Strain	Infection Source	Drug resistance		Chromosomal Mutations		
		Cip MIC (ng/uL)	Cef MIC (ug/mL)	gyrA	gyrB	parC
Pb3	UTI	15.6	4	D678E, A828S	E185D	D475E
Pb15	Respiratory	32000	0.5	**S83L, D87N**, D678E, A828S	S492N, A618T, E656D	**S801**, A108V
Pb35	Blood	32000	128	**S83L, D87N**, A828S	A618T	**S80I, E84V**, A192V, A471G, D475E,

2.2.3 Growth Curves

AMP activity was evaluated using growth curves. Overnight cultures of bacteria to be tested were grown up in MHB with continuous shaking (150 RPM) at 37°C. The overnight cultures were then diluted 1:100 in MHB and experimental peptides were tested at 40 µM in triplicate in a 96 well plate, with the lid left on to prevent evaporation. OD600 was read every 30 min for 24 hrs with continuous shaking using Gen5 software with a BioTek Plate reader. For serial dilution testing of AMPs, a two-fold dilution series was performed to test the range of 40 µM to 5 µM in triplicates.

To generate growth curves, the OD600 over the 24-hr time period was plotted. All y-values in the linear portion of the log phase were $\log_2$ transformed and plotted against time (min). A linest function was used to output the slope and standard error of regression. All growth rates were normalized to the 'No AMP' control treatment but were normalized to the 'WT AMP' samples for graphical representation.

2.2.4 Hemolytic assay

Haemolytic assay performed as per Darnowski *et al*., 2022. Sheep red blood cells (sRBC) were purchased in a 10% suspension from Fischer Scientific (Cat No. 0855876). UyCT3$_{WT}$, UyCT3$_{I5A, W6Y, K10I, F13I}$, and UyCT3$_{I5A, W6E, K10C, F13V}$ were prepared at a concentration of 400 µM in PBS Buffer. 1% Triton X-100 was used as a positive control, PBS as a negative control, and 0.66% DMSO was used as the vehicle control. 75 µL of AMP was added to 75 µL of sRBC in a flat black

clear bottom 96-well plate. The plate was shaken at 37°C for 1 hr. The plate was spun at 1000*xg* for 15 min to collect the pellet, and supernatant was taken and diluted 1:10 with PBS buffer. OD_{414} was read and hemolysis % was determined by (abs sample – abs neg average)/ (abs pos average – abs neg average). Absorbances were taken in triplicates.

2.2.5 Data Analysis

Growth rate data derived from the AMP permutations were manipulated into a 13 x 19 matrix with the WT AMP on the Y-axis and amino acid mutations along the X axis and subjected to Peptide Specificity Analysis (PeSA) analysis to create motifs for a 2nd generation of AMP synthesis (Topcu and Biggar, 2019). A motif is provided based on a certain threshold, which is relative to the positive control (WT AMP). A threshold of 2 SD above the mean 'WT AMP' score was set. This means that mutations that elicit a mean score that is 2 SD above the 'WT AMP' mean score will be used for producing the motif that will go on to create the 2nd generation of AMPs.

2.2.6 2nd generation peptide clustering

Due to the large number of predicted AMPs generated from UyCT3 motif, the list of predicted 2nd generation AMPs was clustered into 100 individual groups that represent the greatest sequence diversity. These clusters were used for evaluation. Each set of peptides are ranked in each cluster by varying

characteristics: charge, charge density, isoelectric point (pI), Instability Index, Aromaticity, Aliphatic Index, Boman Index, and Hydrophobicity. The top-ranking peptide in each group was compiled into a new list, and this list of 100 AMPs is used for further testing.

2.2.7 Pepwheel visualization

Amino acid residue formation for UyCT3 and UyCT3$_{I5A, W6Y, K10I, F13I}$ were visualized using the EMBOSS pepwheel tool. (EMBOSS; **http://emboss.bioinformatics.nl/cgi-bin/emboss/pepwheel**).

2.2.8 Statistical analysis

Statistical analysis was performed using an independent students t-test. Mean values of experimental AMPs are tested against mean WT AMP growth rates. * Denotes p value < 0.05, ** denotes p value < 0.01, *** denotes p value < 0.001.

2.3 Results

2.3.1 Effect of single amino acid mutations on growth inhibition

As a first step towards optimizing indolicidin and UyCT3 against *E. coli,* we performed amino acid permutations. The WT peptide was kept constant, while systematically changing one residue to each of the 19 other amino acids. This resulted in 520 unique peptides (260 for indolicidin and 260 for UyCT3). Each of

these peptides were then tested against the laboratory *E. coli* WT strain MG1655 (K12). Each peptide was initially tested at 40 μM, as this is a typical minimal inhibitory concentration (MIC) for most AMPs (Luna-Rameriz et al., 2013). The growth rate of each peptide was then normalized to the growth rate of the 'WT AMP' condition.

Figure 2.1 shows data from the initial peptide permutation screens of Indolicidin (Fig. 2.1A-B) and UyCT3 (Fig. 2.1C-D). From the UyCT3 screen, 118 peptide mutations decreased bacterial growth, while 129 peptides increased bacterial growth compared to WT UyCT3. For Indolicidin, 125 peptide mutations decreased bacterial growth, while 122 peptides increased bacterial growth compared to WT Indolicidin. Notably, any amino acid substitution at Lysine 5 (i.e., K5) of Indolicidin decreased growth by 2 to 7-fold (Fig. 2.1A), highlighting that any mutations in this position influences the AMP potential of this peptide.

Peptide Specificity Analyst (PeSA) software was used to generate a sequence motif that represents all AMP mutations that increased the potency of either Indolicidin (Fig. 2.1B) or UyCT3 (Fig. 2.1D) peptides; the threshold cut-off for the motif was based on +2SD above the mean 'WT AMP' score (2.91 and 1.069 for Indolicidin and UyCT3, respectively). Many of the residues found in the original AMP sequence are held constant in the motifs, but a large array of amino acid families can also be identified. Each amino acid residue is colored based on the legend provided in Figure 2.1, with many tolerable amino acids being hydrophobic in nature.

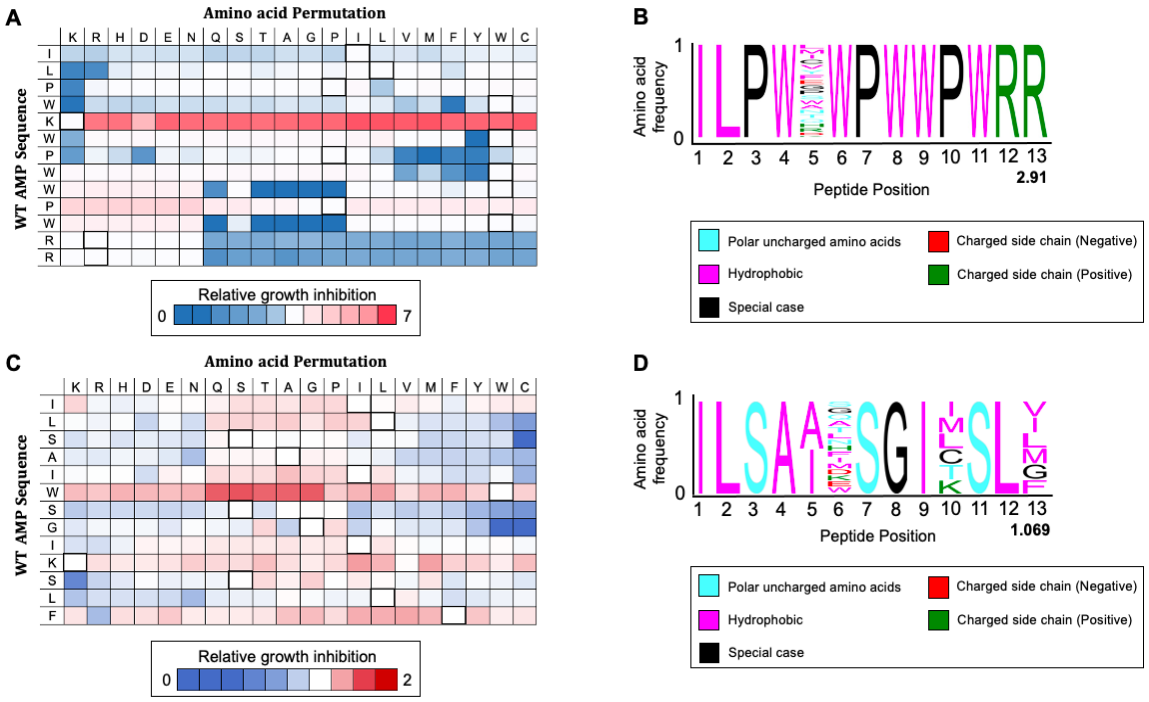

Figure 2.1. Amino acid permutations show increased antimicrobial activity. **(A)** Growth rate detection through single amino acid permutation of Indolicidin. **(B)** owth rate detection through single amino acid permutation of UyCT3. Relative growth inhibition is shown with each respective bar. A blue hue represents mutations that did not result in any growth inhibition, while red represents mutations that performed better than the WT peptide. Any boxes colored white show inhibition like the WT. All points are normalized to the substitution that results in the WT AMP (showed in bolded boxes). Motifs are shown in (C) for Indolicidin and (D) for UyCT3. Amino acid frequencies are shown on the y axis, with the larger a residue is, the more important its placement is for inhibition.

2.3.2 Clustering of candidate AMPs using sequence motifs

PeSA was used for the generation of initial sequence motifs that increased AMP function (decreased MG1655 growth rate). To generate the second generation of peptides, PeSA was then used to output every combination of sequences that are encoded within each motif. This resulted in a total of 20 and 1440 peptides for Indolicidin and UyCT3, respectively. Given the high number of combinatorial peptides based on the UyCT3 motif, the 1440 peptides were clustered into 100 discrete groups for testing; these clusters were ranked based on peptide characteristics (Charge, Charge Density, pI, Instability, Aromaticity, BomanInd, and Hydrophobicity). This clustering allowed us to create a tangible number of diverse 100 UyCT3-derived candidates for further testing.

2.3.3 Growth inhibition by 2nd generation AMPs

A total of 120 peptides representing our 2nd generation of AMPs were synthesized and tested against MG1655 at 40 μM, and their growth rates are shown in Figure 2.2. Indolicidin provided 20 different AMPs based off the motif, and only 4 of those showed significant decreased growth relative to indolicidin. As for UyCT3, 6 out of the 100 predicted AMPs significantly decreased growth compared to UyCT3. Notably, these peptides differ from the first set of peptides tested (Fig. 2.1) as they contain at least one or more amino acid mutations and are not derived directly from the WT sequence. While 120 peptides were tested in total, only peptides that display significant growth inhibition are shown. The growth rates of the 120 peptides are shown in Table A1 and Table A2 in Appendix A for UyCT3

and Indolicidin, respectively. Only peptides that showed p value < 0.05 were chosen to move further. These peptides were then chosen to move forward for further testing, with their peptide sequences shown in Table 2.2.

Table 2.2. AMP candidates from the 2nd generation screen.

Peptide Name	Sequence
$Indo_{K5A}$	ILPWAWPWWPWRR
$Indo_{K5C}$	ILPWCWPWWPWRR
$Indo_{K5D}$	ILPWDWPWWPWRR
$Indo_{K5L}$	ILPWLWPWWPWRR
$UyCT3_{I5A,\ W6Y,\ K10I,\ F13I}$	ILSAAYSGIISLI
$UyCT3_{I5A,\ W6E,\ K10C,\ F13V}$	ILSAAESGICSLV
$UyCT3_{I5A,\ W6Q}$	ILSAAQSGIKSLF
$UyCT3_{I5A,\ W6Y,\ K10M,\ F13V}$	ILSAAYSGIMSLV
$UyCT3_{W6T,\ K10M}$	ILSAITSGIMSLF
$UyCT3_{I5A,\ W6M,\ K10T}$	ILSAAMSGITSLF

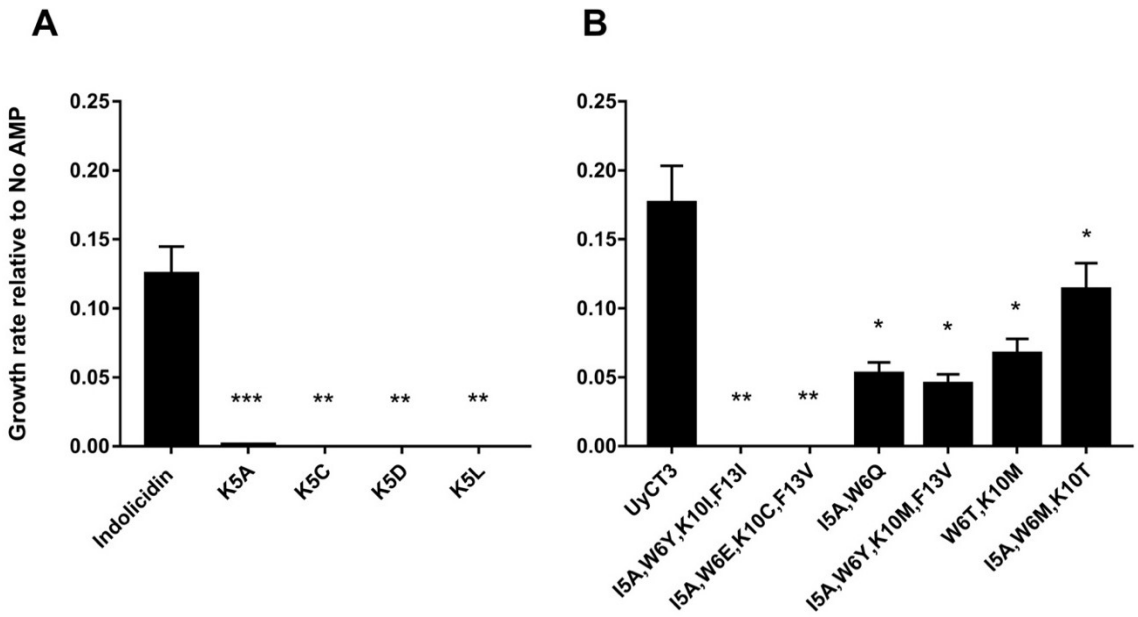

Figure 2.2. **2nd generation peptides show better growth inhibition than WT AMP.** Growth rate of the 2nd generation of peptides (A) against Indolicidin and (B) against UyCT3 in MG1655 tested at 40 μM. * for p value < 0.05, ** for p value < 0.01, and *** for p value < 0.001. All growth rates were normalized to No AMP treatment, and statistics were compared to the WT peptide. Error bars show the standard error of regression.

2.3.4 Growth inhibition of clinical strains by 2nd generation AMPs

To give insight into the clinical relevance of our chosen peptides, three strains of *E. coli* (AMR profiles shown in Table 2.1), Notably, the Indolicidin 2nd generation AMPs were found to display a broad range of effects on these clinical strains (Fig. 2.3A). Specifically, there is greater effect of $Indo_{K5A}$ and $Indo_{K5C}$ against strains pb3 and pb35, with a reduced but still significant effect on pb15. The Indolicidin-derived AMPs $Indo_{K5D}$ and $Indo_{K5L}$ gave an equivalent response across all three strains and were chosen for further characterization. For UyCT3-derived AMPs, only three out of the nine peptides significantly decreased growth across all three strains, with $UyCT3_{I5A,\ W6Y,\ K10I,\ F13I}$ and $UyCT3_{I5A,\ W6E,\ K10C,\ F13V}$ displaying highly significant growth inhibition ($p < 0.01$) (Fig. 2.3B).

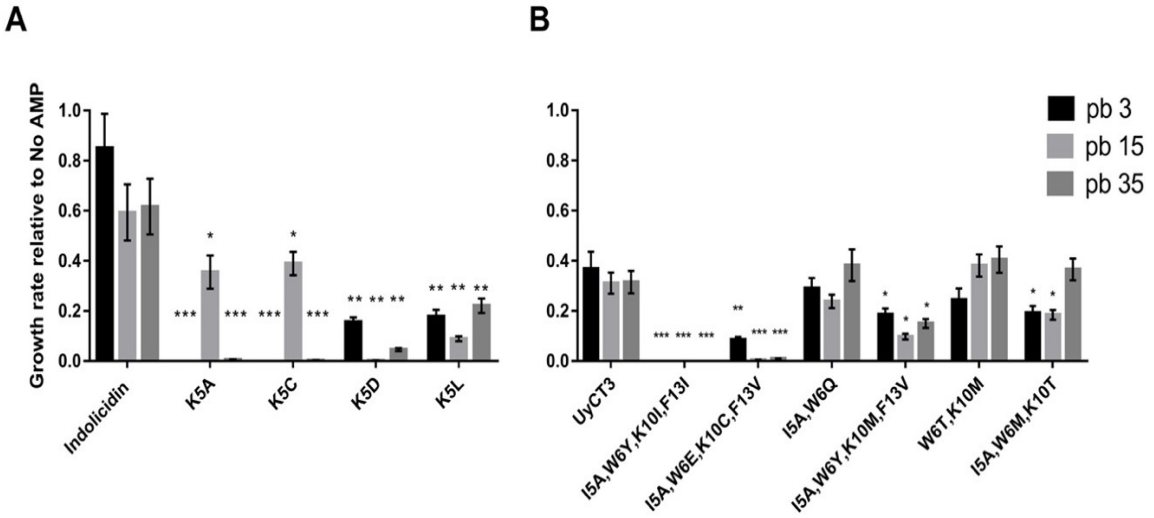

Figure 2.3. **AMPs show broad inhibition across three clinical strains.** AMPs shown in Table 2.2 originating from (A) Indolicidin and (B) UyCT3 tested against strains pb3 (black), pb15 (light grey), and pb35 (dark grey). All AMPs tested at 40 μM. * for p value < 0.05, ** for p value < 0.01, and *** for p value < 0.001. All growth rates were normalized to No AMP treatment, and statistics were compared to the WT peptide. Error bars show the standard error of regression.

2.3.5 Dose-response of candidate AMPs

We generated dose-response curves for our candidate AMPs by performing a serial dilution ranging from 5 to 40 μM (Fig. 2.4). WT AMPs were also tested in the same concentration range. As expected, all candidate AMPs inhibited growth at 40 μM. $Indo_{K5D}$ significantly inhibited bacterial growth at concentration down to 10 μM in pb15, in comparison to $Indo_{WT}$, but only down to 20 μM in pb3. $Indo_{K5L}$ inhibited pb35 significantly at 20 μM. $Indo_{WT}$ inhibited pb35 and pb15 in a concentration dependent manner, while pb3 growth was not inhibited across the concentrations tested. $Indo_{K5D}$ is the most promising derivative since it inhibits strains pb15 at 10 μM and pb3 at 20 μM.

Across all three strains, UyCT3 and its derivates showed antimicrobial activity. $UyCT3_{WT}$ was inhibited at 40 μM for pb3 and pb35 but showed a linear range of inhibition for pb15. $UyCT3_{I5A,\ W6Y,\ K10I,\ F13I}$ showed to be significant against pb35 and pb3 at concentrations greater than or equal to 10 μM. All three UyCT3 tested peptides have a similar response to pb15, with $UyCT3_{I5A,\ W6Y,\ K10I,\ F13I}$ and $UyCT3_{I5A,\ W6E,\ K10C,\ F13V}$ inhibiting bacterial growth significantly at 40 μM. $UyCT3_{I5A,\ W6Y,\ K10I,\ F13I}$ is the most promising derivative because of its ability to inhibit growth at concentrations of 5-10 μM of most strains.

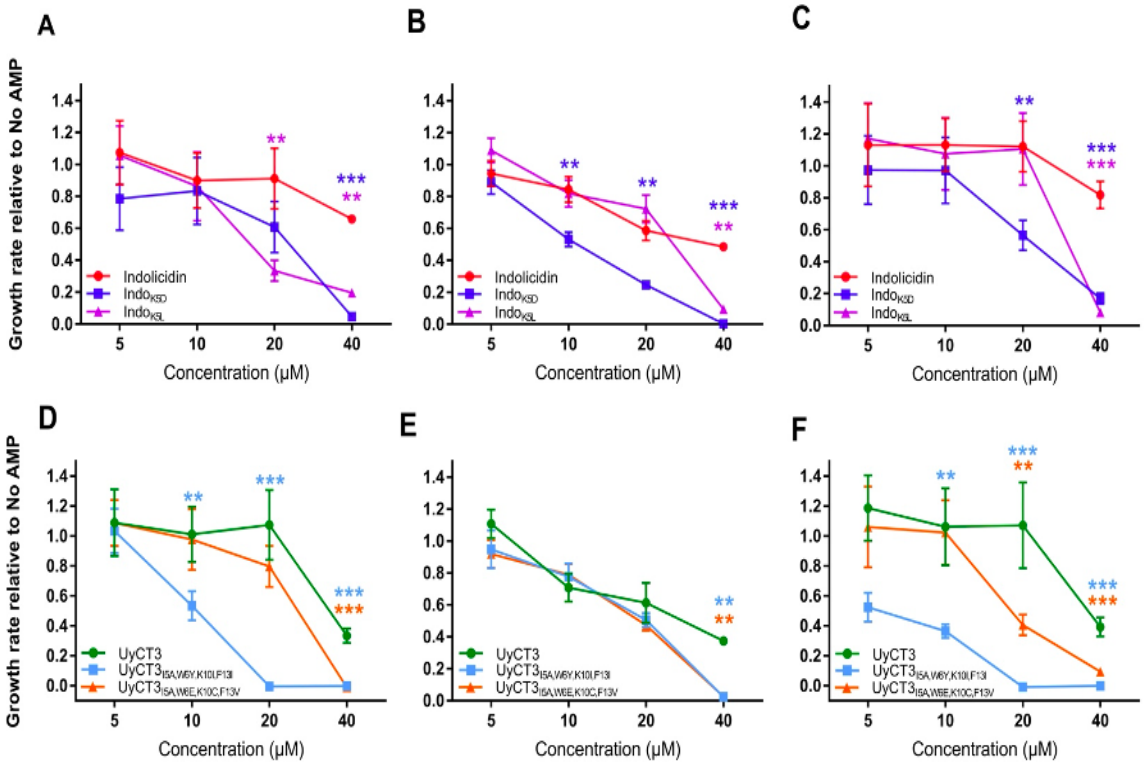

Figure 2.4. Serial dilution of AMPs against clinical strains exhibits different range of inhibition. (A), (B), and (C) show Indolicidin variants tested against pb35, pb15, and pb3, respectively. (E), (F), and (G) show UyCT3 variants tested against pb35, pb15, and pb3, respectively. Legend is shown in the bottom left. * for p value < 0.05, ** for p value < 0.01, and *** for p value < 0.001. All growth rates were normalized to No AMP treatment, and statistics were compared to the WT (either Indolicidin or UyCT3) peptide. Error bars show the standard error of regression.

2.3.6 α-helical mapping of UyCT3$_{I5A, W6Y, K10I, F13I}$

UyCT3$_{I5A, W6Y, K10I, F13I}$ was further investigated to explore why it might work better at inhibition of bacterial growth compared to UyCT3. EMBOSS pepwheel was used to visualize the formation of amino acids in our peptide sequence to identify regions of hydrophobicity and hydrophilicity. Aliphatic residues are marked with blue squares, hydrophilic residues are shown in red diamonds, positively charged residues with black octagons, and hydrophobic residues in purple font. Figure 2.5A shows UyCT3, while Figure 2.5B shows UyCT3$_{I5A, W6Y, K10I, F13I}$. With the mutations made to create this new peptide, we are replacing residues to amino acids that have aliphatic characteristics with branched side groups. We still maintain the very heavily hydrophilic left side of the helical peptide with its abundant serine residues, which creates a more amphipathic peptide.

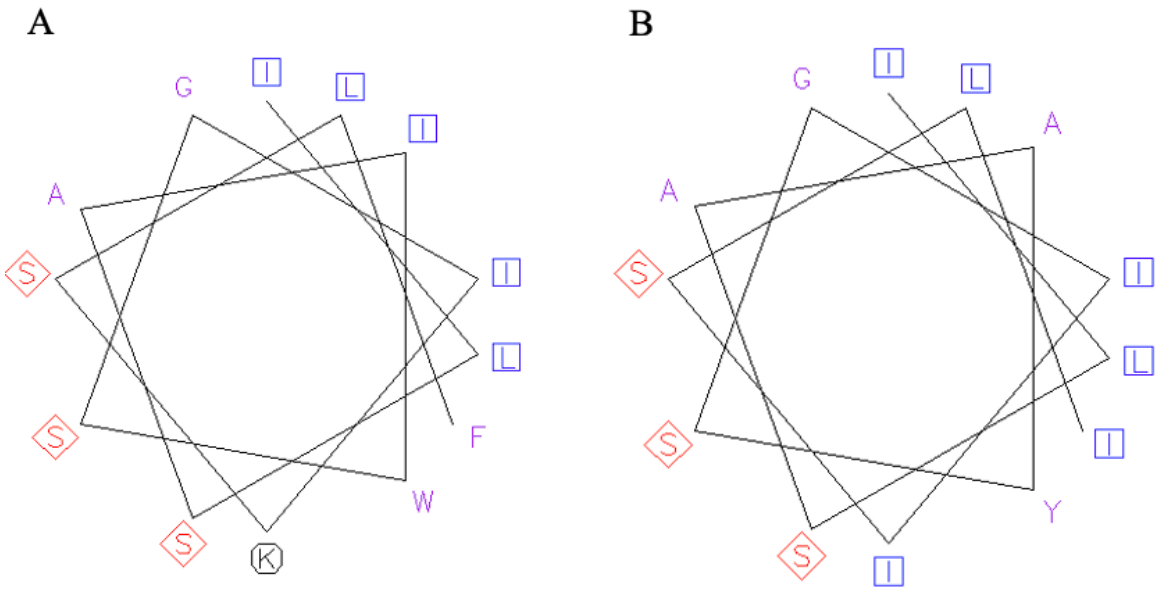

Figure 2.5. UyCT3$_{I5A, W6Y, K10I, F13I}$ results in more amphipathic peptide than UyCT3$_{WT}$. (A) shows the pepwheel for UyCT3$_{WT}$ and (B) shows the pepwheel for UyCT3$_{I5A, W6Y, K10I, F13I}$. Image generated using EMBOSS Pepwheel software. Aliphatic residues are marked with blue squares, hydrophilic residues are marked in red diamonds, and positively charged residues with black octagons, and hydrophobic residues in purple font.

2.3.7 Hemolytic activity of UyCT3 and its variants

As a preliminary screen for cytotoxicity, hemolytic activity UyCT3, UyCT3$_{I5A, W6Y, K10I, F13I}$, and UyCT3$_{I5A, W6E, K10C, F13V}$ were tested against sheep red blood cells (sRBC) (Figure 2.6). HC_{50} values were found for UyCT3 against human erythrocytes at 20 μM (Ramirez *et al.,* 2014) but to cast a wide net, concentrations of 200 μM to 3.125 μM were used for the assay across all three peptides. At 200 μM, UyCT3$_{I5A, W6E, K10C, F13V}$ showed close to 10% hemolysis activity, while UyCT3 and UyCT3$_{I5A, W6Y, K10I, F13I}$ showed less than 5%.

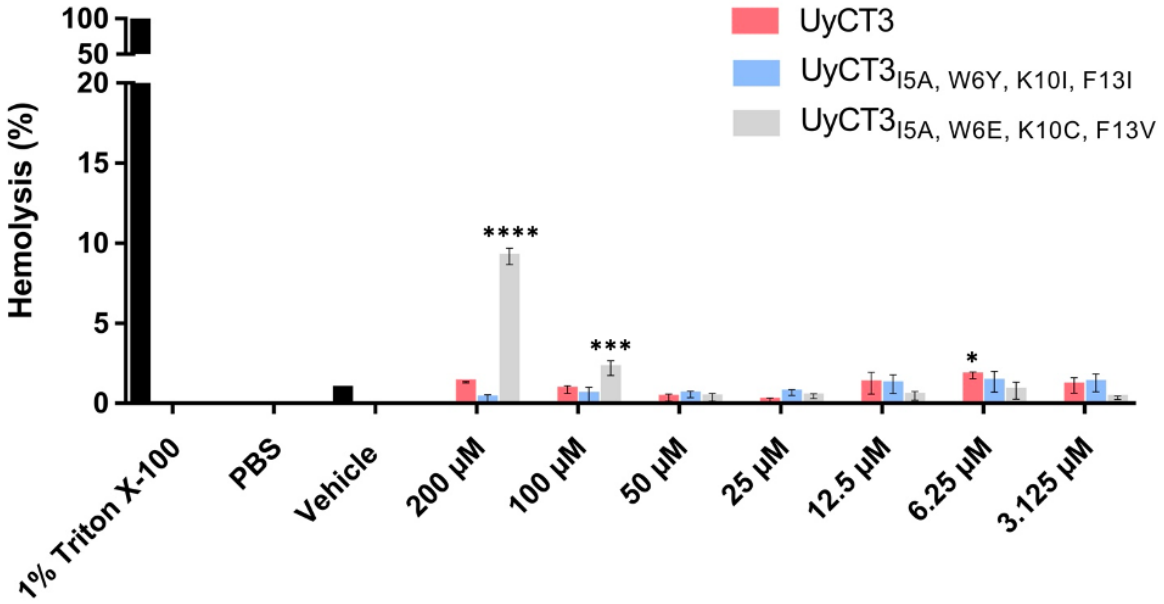

Figure 2.6. Hemolytic activity of predicted AMPs. Hemolysis percentage of UyCT3, UyCT3$_{I5A, W6Y, K10I, F13I}$, and UyCT3$_{I5A, W6E, K10C, F13V}$ against sheep red blood cells. A range of 200-3.125 µM was tested. Error bars show standard deviation. Significance is tested against the vehicle control.

Discussion

While there have been many advances in antimicrobial therapeutics and combatting AMR in the last decade, there is still a need to find new therapeutics active against resistant resistance or emerging pathogens. The process of finding new antibiotics is costly, as most are found through natural sources (plants, fungi, etc.) (Dutescu and Hillier, 2021). Most known AMPs are found abundantly in nature, having come from various animal sources (Uddin *et al*., 2021). These AMPs have evolved against non-human borne pathogens and may not show much antimicrobial activity against human pathogens. We used permutations of two naturally occurring AMPs to assess how differing amino acid makeup affects antimicrobial activity.

Similar permutation studies of AMPs have been reported, but they were done rather differently than the scope of this study (Koch *et al*., 2022; Kumar *et al*., 2019; Mishra *et al*., 2020). Those studies either implement a sliding window motif (Mishra *et al*., 2020), certain amino acid mutations at certain positions (Kumar *et al*., 2019), or the intracellular expression of AMPs for growth inhibition (Koch *et al*., 2022). Our approach differs from the previously mentioned studies in that we permutated our AMPs at each residue with all 20 amino acids across the length of the peptide to observe changes in AMP activity due to individual mutations. This allows a more in-depth look at how each mutation effects bacterial growth. This technique is much better at looking at membrane disruption than if AMPs were expressed intracellularly, such as Koch *et al*., 2022.

Through systematically evolving two known AMPs, Indolicidin and UyCT3, we developed 4 AMPs that inhibit bacterial growth against human pathogens with more potency than their wild-type counterparts. Out of these 4 AMPs, $UyCT3_{I5A, W6Y, K10I, F13I}$ shows the most promise as the least toxic towards sheep red blood cells. This AMP shows very little hemolytic activity, and inhibited growth of MDR pathogens at concentrations as low as 5 μM compared to $UyCT3_{WT}$.

Mutating position K5 of indolicidin to any other amino acid showed a drastic change in antimicrobial activity, even when mutating to arginine, a residue with similar biophysical characteristics (Fig. 2.1A). Often, mutations of lysine to arginine do not cause drastic effects on peptide activity since both amino acids carry a positive charge (Cutrona *et al.,* 2015). Though the nature of most AMPs is cationic, there is a preference for guanidinium groups in arginine rather than the amine group observed in lysine (Cutrona *et al.,* 2015). Smirnova *et al*., 2004 did select permutations on indolicidin and evaluated minimal inhibitory concentrations (MICs) against various strains, including *E. coli* M17. Of these permutations, $Indo_{K5A}$ was tested and showed a reduction in the MIC from 2 μM to <1.5 μM for the wild type AMP and mutant, respectively. A reduction in the MIC correlates to a better acting antimicrobial. However, it did result in increased hemolytic activity.

UyCT3 permutation analysis showed important residues for bacterial growth inhibition. Of particular importance, position W6 had the most leniency for mutations. When mutating this position to either glutamine (Q), serine (S), threonine (T), alanine (A), or glycine (G) growth inhibition increased (Fig. 2.1C). These amino acids are hydrophilic, and with their mutation, this creates a more

amphipathic AMP. Amphipathic refers to a molecule containing both a hydrophobic and hydrophilic side. Amphipathic AMPs are abundantly cited being found in natural sources, and many AMPs are deemed amphipathic such as cecropins, magainins, thionins, defensins, and cathelicidins (Chrom *et al*., 2020).

Our top candidate AMPs derived from either Indolicidin or UyCT3, were tested against the three clinical strains of *E. coli.* WT UyCT3 AMP was better at inhibiting growth of the three strains than WT Indolicidin (Fig. 2.3). As discussed earlier, Indolicidin works at inhibition of DNA synthesis. It binds directly into the abasic site of DNA and cross-links single or double stranded DNA (Hsu *et al.,* 2005; Huan *et al.,* 2020; Marchand *et al*., 2006). Interestingly, the chosen clinical strains all contain mutations in both gyrase A and B. Gyrase proteins play a main role in the super coiling of DNA. It has previously been shown by Bagel *et al*. (1999) that strains that contain gyrA D87N/S83I mutations alongside a parC S80I mutation (such as in pb15 and pb35 strains) lead to increase levels of supercoiling. Increased supercoiling results in lower levels of replication, which results in a reduced growth rate. It is then theorized that any lower growth rate from Indolicidin treatments for pb3, pb15, or pb35 vs. MG1655 are due to strain specific mutations and not necessarily AMP-mediated inhibition. However, upon mutation of position K5 of indolicidin to either alanine(A), cysteine(C), aspartic acid(D), or leucine(L) bacteria growth decreased across all strains. There were not variations in the effects of UyCT3 on pb3, pb15, or pb35 and I believe that is due to the mechanism of action that is proposed for UyCT3. It works by disrupting bacterial membranes, so variations are not entirely expected.

To observe the effect of concentration of our AMPs on our clinical strains, a serial dilution was performed for the candidates selected (Figure 2.4). UyCT3$_{I5A, W6Y, K10I, F13I}$ is the most promising derivative because of its ability to inhibit growth at concentrations of 5-10 μM of most strains. Indo$_{K5D}$ is the most promising derivative since it inhibits strains pb15 at 10 μM and pb3 at 20 μM.

To investigate why our quadruple mutant UyCT3$_{I5A, W6Y, K10I, F13I}$ might be inhibiting bacterial growth better than WT UyCT3, we plotted the alpha-helix conformation using EMBOSS Pepwheel (Fig. 2.5). EMBOSS Pepwheel visualization allows us to also look at the distribution of amino acid residues in the context of peptide structure. Interestingly, mutations in UyCT3$_{I5A, W6Y, K10I, F13I}$ result in a more hydrophobic region on one side (Fig. 2.5B) the right side than the WT peptide. Accompanied by the abundance of serine residues on the opposite side, this leads to the creation of a more amphipathic AMP.

Amphipathic AMPs are known to work by one of three models, 1) barrel pore, 2) toroidal pore, and 3) carpet model (Langenegger *et al*., 2019). In the barrel pore model, multiple AMPs oligomerize and insert themselves perpendicularly in the membrane. This forms a pore where the hydrophilic region of the AMPs orients themselves towards the inside of the pore. In the toroidal pore, it is similar to the barrel pore model with the exception that there are interactions between lipid head groups between AMPs. Finally, the carpet model is unique in that creates peptide-micelle formation and formation of holes in the membrane (Langenegger *et al*., 2019). Since UyCT3 is proposed to create a helical membrane in the channel of

the bacterium, such mutations may encourage channel formation leading to loss of cell rigidity (Almaaytah and Albalas, 2014; Luna-Rameriz *et al.,* 2013).

It is also important to look at the impact of permutation on the oligomerization of AMPs in solution. Fig 2.5A shows UyCT3$_{WT}$ which has a solvent exposed lysine residue. Fig 2.5B shows the mutated AMP, UyCT3$_{I5A, W6Y, K10I, F13I}$, which loses the lysine residue. This loss of positive charge might allow for better oligomerization due to no positive charge repulsions between peptide structures in pore formation. This is termed the coulomb repulsion, which is the repulsive force between two positive or two negative species (Norouzy *et al*., 2015). The coulomb repulsion is a driving force for the determination of biological peptide activity.

A hemolytic assay was performed to measure toxicity towards mammalian cells. Hemolysis assays are implemented as a tool for the viability of AMPs as therapeutics, as it allows for the screening of toxic compounds against mammalian cells (Greco *et al*., 2020). At 200 μM, UyCT3$_{I5A, W6E, K10C, F13V}$ showed close to 10% hemolysis activity, while UyCT3 and UyCT3$_{I5A, W6Y, K10I, F13I}$ showed less than 5%. At clinically relevant concentrations, UyCT3 and UyCT3$_{I5A, W6Y, K10I, F13I}$ showed the least toxicity towards sRBC. Even though UyCT3$_{I5A, W6Y, K10I, F13I}$ takes on a more amphipathic structure, it appears to have low affinity for mammalian membranes.

We have optimized an AMP that is more potent than its WT counterpart at a 3-fold concentration difference. Further, this novel UyCT3$_{I5A, W6Y, K10I, F13I}$ AMP was able to inhibit growth of various clinical strains, which have a very abundant AMR profile and known resistance to antibiotics. This systematic AMP design was accomplished using a permutation library of a known AMP sequence. With the

success of this approach *in vitro*, this application can be implemented to develop new AMPs, examining how systematic permutating and *in vitro* evolution of existing AMP sequences might lead to better antimicrobial activity.

Future directions can be to look at the membrane disruption of *E. coli* with UyCT3$_{I5A,\ W6Y,\ K10I,\ F13I}$. This has been done before with the use of unilamellar vesicles that contain carboxyfluorescein that are quenched when inside the vesicle and fluoresce outside of it. Upon treatment with AMPs, the vesicles burst open and release the carboxyfluorescein (Mercer *et al*., 2020). Due to the amphipathic nature of the optimized AMP, there is the possibility that it will have affinity for bulky proteins in serum.

Since the mechanism of UyCT3 is not entirely known in detail, there maybe be intracellular targets of the AMP. Two-dimensional PAGE is a robust technique for the analysis of protein composition in biological samples (O'Farrell, 1975). The technique firstly looks at separating proteins by their isoelectric points, followed by a separation of mass (O'Farrell, 1975). Through treatments with AMPs, there could be variances in the expression of proteins compared to a control group. There are disadvantages to this in that there might be a masking of large molecular weight proteins that are found in bacterial membranes.

Another technique to look at interaction of proteins under experimental conditions is the use of mass spectrometry. Mass spectrometry measures the masses of charged species, and the identity of the proteins can be identified. You can also interpret chemical modifications, and the protein structure (Olshina and Sharon, 2016). Upon AMP treatment, cell samples can be collected and run to

identify any key protein that are abundant, either overexpressed or underexpressed.

Chapter 3:

Development of peptide based β-lactamase inhibitors against TEM-1 using an Orientated Peptide Array Library and evaluating inhibition using nitrocefin cleavage

Since their discovery in 1929, β-lactams have been successful in the treatment of bacterial infections. Over time, the structure of β-lactams was evolved and chemically substituted to allow for broad antimicrobial activity. The evolving structure of this diverse class has drastically changed the course of medicinal sciences (Beadle *et al*., 2001).

β-lactams are one of the three largest classes of antibiotics, and their mechanism of action and antibacterial activity have been heavily reviewed. Penicillin was the first β-lactam discovered, and over the years the diverse array of chemical compounds has expanded to cover four different groups. All four of these groups of β-lactam are currently in clinical use: penicillins, cephalosporins, carbapenems, and monobactams. β-lactam activity is known to derive from the presence of the structural similarity to the D-Ala-D-Ala moiety of the peptidoglycan stem pentapeptide, which is the substrate for Penicillin Binding proteins (PBPs) (Tipper and Strominger, 1965). This similar structure is distinguished as the β-lactam amide bond and the adjoining carboxylate groups (Kapoor *et al*., 2017).

It is well known that penicillin binding proteins (PBPs) are necessary for cell wall synthesis in both gram-negative and gram-positive bacteria. PBPs polymerize and modify the peptidoglycan layer of bacterial cell wall, and thus help create the morphology of the cellular exoskeleton. Peptidoglycan is made up of glycan chains of alternating sugar monomers, *N*-acetylglucosamine and *N*-acetylmuramic acid that are crosslinked by short peptides. β-lactams can stop this process by the irreversible alkylation of PBPs (Beadle *et al*., 2001). This leads to the inactivation of PBPs, and thus to defects in the cell wall structure and irregularities in the shape

of the cell (Beadle *et al*., 2001; Tipper and Strominger, 1965). This mechanism involves interaction between the nucleophilic serine residue of the PBP and the β-lactam amide bond (Kapoor *et al*., 2017). This mechanism is simplified and shown in Figure 3.1.

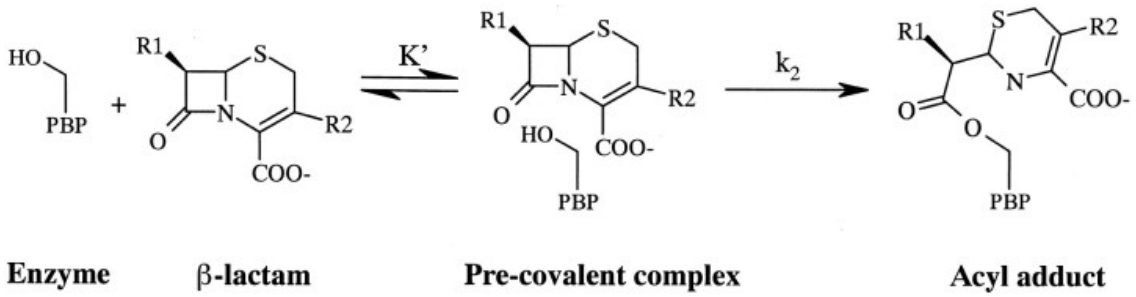

Figure 3.1. Enzyme acyl formation of PBPs to β-lactam antibiotics. Adapted from Beadle *et al*., 2001.

The use of β-lactam antibiotics has led to the emergence of resistance pathways to overcome the efficacy of these drugs. Resistance can be acquired by various methods, including downregulation of porin proteins needed for β-lactam intake, mutations of targets (PBPs in this case), and the production of enzymes that facilitate the breakdown of β-lactams (King *et al*., 2017; Tooke *et al*., 2019).

Here, I focus on β-lactamases as the most clinically relevant resistance mechanism. β-lactamases are a class of enzymes that hydrolyze the β-lactam amide bond and thus lead to the inactivity of the antibiotic and are found in both gram-negative and gram-positive bacteria (Alaybeyoglu *et al.,* 2017; Tooke *et al*., 2019). β-lactamases can be characterized into four classes, termed A, B, C, and D, with further sub-categorization by sequence motif or hydrolytic mechanisms. Classes A, C, and D are termed active serine enzymes (serine β-lactamases, SBLs), and class B are termed zinc metalloenzymes (metallo-β-lactamases, MBLs) (Tooke *et al*., 2019).

Massova and Mobashery, 1998 showed that SBLs are related to PBPs, sharing a motif of Ser-Xaa-Xaa-Lys, which employs a serine mechanism like PBPs. Shown in Figure 3.2 is a graphical representation of the serine mediated breakage of the β-lactam amide bond. Fig 3.2(a) shows the activation of the serine residue found on the SBL by a nearby basic residue. Once activated, the nucleophilic serine attacks the amide carbonyl carbon (denoted by C7) which results in an acyl enzyme formed (shown in Fig 3.2(c)). Another base is used to deprotonate a water molecule, which can then act as a nucleophile and attack the carbonyl of the newly formed acyl enzyme complex.

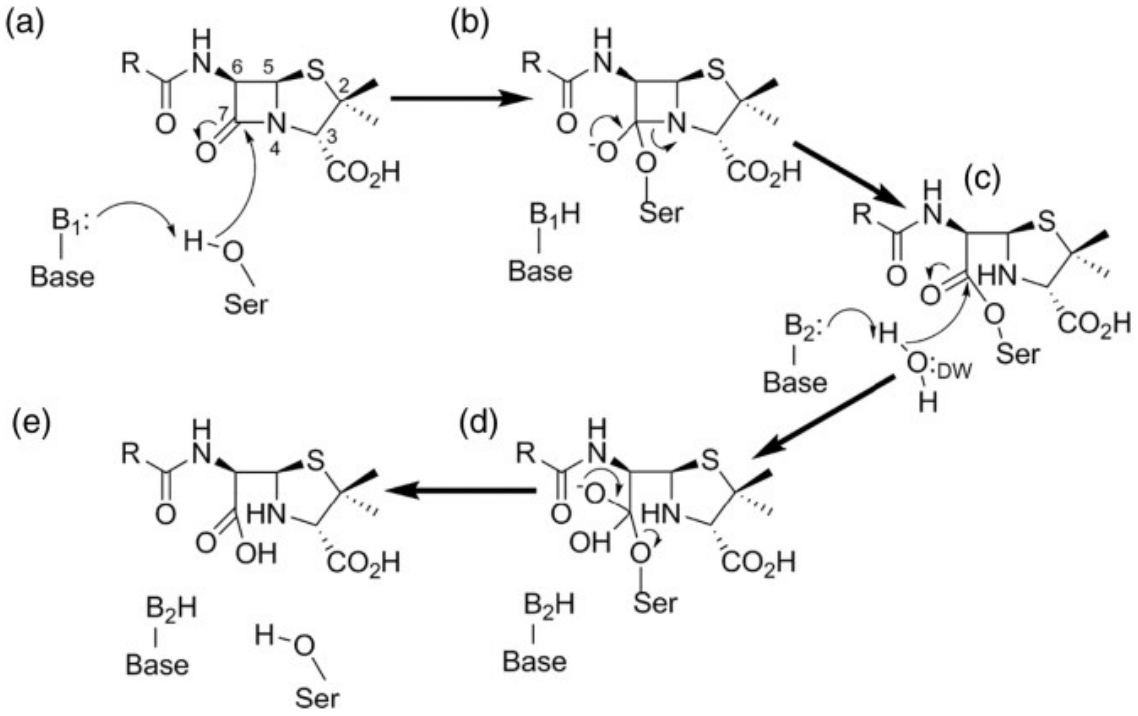

Figure 3.2. Serine β-lactamase mechanism of action. Figure from Tooke *et al*., 2019.

With the increasing prevalence of resistance towards β-lactams, there has been an expanding market of β-lactamase inhibitors (BLIs) (Carcione *et al*., 2021; Tooke *et al*., 2019). BLIs are small chemical compounds that are co-administered with β-lactam antibiotics and are intended to overcome BL-mediated resistance (specifically SBLs). Inhibition of SBLs allows for administered antibiotics to be bioavailable for bacterial inhibition. Discovery of BLIs started in the 1970s, upon emergence of TEM-1 producing bacteria (Bush and Bradford, 2016). Clavulanic acid, sulbactam, and tazobactam are the 3 major BLIs that are on the market currently and have been shown to be effective against various BLs. Other BLIs include, but are not limited to, vaborbactam, relebactam, and avibactam. These BLIs are taken alongside β-lactam antibiotics as combinatory therapy to help reduce infections in patients. These combinations have been shown as viable treatments for both community and hospital associated infections by pathogens producing β-lactamases.

BLIs that are being used currently are starting to show a very low spectrum of activity against emerging β-lactamases. These BLIs are structurally like β-lactam antibiotics and react similarly as well by interaction of the key serine residue. The use of BLIs that mimic β-lactam antibiotics has resulted in selected pressure resistance to BLIs (Rudgers *et al*., 2001). A study looked at clavulanic acid/amoxicillin resistance in site directed mutagenesis of the primary serine residue that is found in the β-lactamase TEM-1. They showed that a triple mutant of TEM-1 (E104K, S268G, and N276D) had an almost 8-fold increase in the K_i of clavulanic acid, which indicates a lower affinity for the inhibitor (Vakulenko and

Golemi, 2002). With the increase of resistance and mutations of known BLs, there is a necessity for the development of BLIs that do not take on the canonical structure of those currently found (Alaybeyoglu *et al*., 2017; Grigorenko *et al*., 2017).

BLIs can work by various mechanisms. If they take on the structure of β-lactam antibiotics, they typically interact with the active site of SBLs and create irreversible acyl-enzyme interactions. Through this mechanism, BLs can no longer bind β-lactams and leave them inactive. BLIs can bind onto BLs with high affinity and not allow for antibiotic substrates to be cleaved through an acyl-enzyme formation. They can also inactivate the enzyme through other means of binding, either at or away from the active site (Bush and Bradford, 2016).

While β-lactam antibiotics analogs have been typically used as BLIs, peptides may also be used to target various BLs (Brown and Palzkill, 2010; Huang *et al*., 2003; Rudgers *et al.*, 2001). These peptides are either discovered by permutation of known peptide inhibitors or through a broad-scoping approach, such as phage library display or peptide arrays. Peptide arrays have been used as large screening approaches for the discovery of many different therapeutics. This involves the synthesis of peptides on a planar cellulose support, which can be used for big screening of molecular binding events (Reineke *et al*., 2001). Combinatory peptide libraries have been used for analyzing binding or substrate identification of various protein domains (Ahmed *et al*., 2010; Rodriguez *et al.*, 2004).

An orientated peptide array library (OPAL) was used for this study. OPAL arrays are a peptide array that allow examination of the interaction between

peptides and proteins. A schematic is shown in Figure 3.3. A desired peptide length is chosen, and from there one amino acid in the sequence is fixed while the rest of the sequence is denounced as degenerate. Degeneracy refers to an equimolar mix of all amino acids (excluding Cysteine) (Rodrigeuz *et al*., 2004). To allow for better binding capabilities, the peptides are attached to the cellulose with the use of a linker amino acid, typically aminocaproic acid. It should be noted that the application of this technique is utilized to identify peptide binders, and not inhibitors. Candidate peptides are then tested to assay inhibition of recombinant β-lactamase TEM-1.

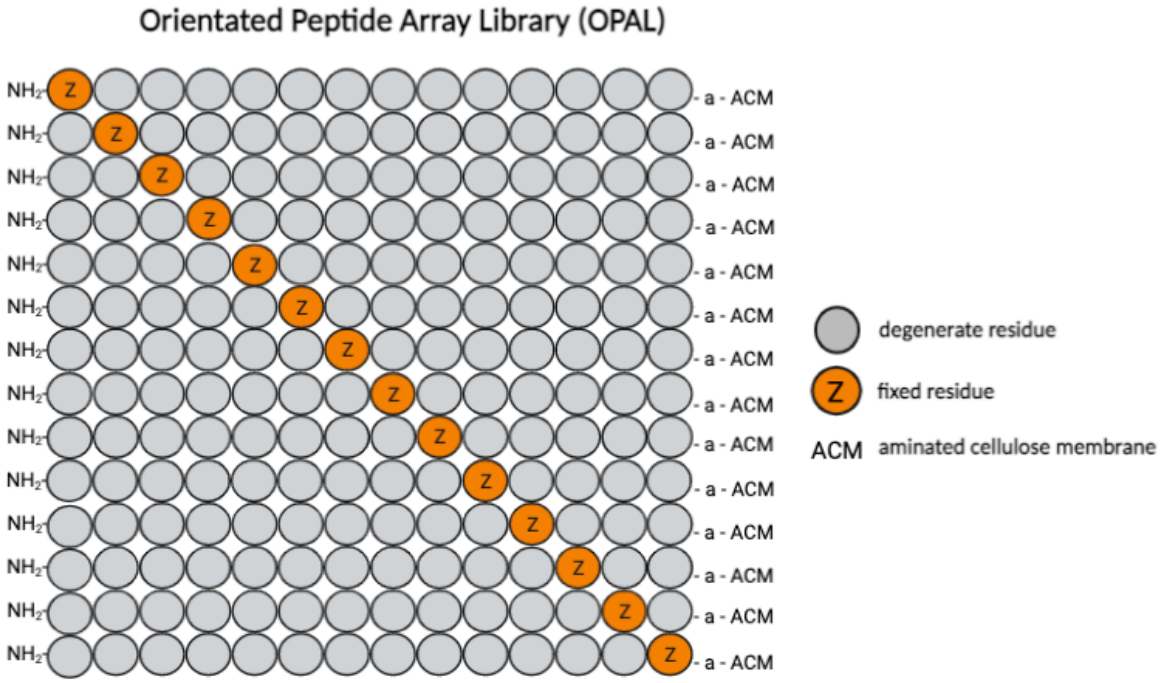

Figure 3.3. Schematic of OPAL design. Generation of Orientated peptide array library on aminated cellulose membrane. 14-mer peptides were synthesized with fixed residues (shown in orange Z circle) that are flanked with residues that originated from an equal molar mix of 19 amino acids except for cysteine.

For this Chapter, I used an OPAL array that contains 14-mer peptides with degenerate sequences to develop inhibitors of the TEM-1 β-lactamase. TEM-1 is a class A β-lactamase that is encoded by *bla*$_{TEM-1}$. TEM-1 was first isolated from *E. coli* in a blood culture from a patient in Greece (Medeiros, 1984), and is one the most common plasmid-encoded β-lactamase in gram negative bacteria.

With the use of recombinant His-tagged TEM-1, I was able to assess binding of the peptide candidates using chemiluminescence detection. Distinct peptide sequences were then generated from the OPAL array, and peptide candidates were assessed for inhibition through enzymatic assays and nitrocefin.

Materials and Methods

3.2.1 Strains

BL21 DE3 was used for protein expression, while DH5α was used for plasmid amplification.

3.2.2 TEM-1 purification

The N-terminal His tagged TEM-1 β-Lactamase gene was a gift from Niels Geijsen (Addgene plasmid # 62729; http://n2t.net/addgene:62729 ; RRID:Addgene_62729). Recombinant His-TEM-1 was purified as per D'Astolfo *et al*., 2015. Briefly, *Escherichia coli* BL21 DE3 cells containing the construct were grown at 37°C with shaking at 200 RPM in LB broth containing 1% glucose and 100 ug/mL Ampicillin. Overnight culture was diluted 1:100 and grown up to an OD_{600} of ~0.5. Expression was induced using 1 mM isopropyl β-D-1-

thiogalactopyranoside (IPTG) for 18 hrs at 16°C. The following day, bacterial cultures were spun down at 3000 RPM at 4°C. Cells were lysed in the presence of 1 mg/mL chicken egg lysozyme, 1 uM E64 in 50 mM NaHPO4. Cell lysate was spun at 18000 RPM for 45 min at 4°C to collect bacterial pellet. Supernatant was taken and diluted 1:1 with 50 mM NaHPO4 buffer containing 5 mM imidazole and incubated with 500 μL bead volume of Ni-NTA Beads for 2 hrs at 4°C. After bead incubation, lysate was spun down and a fraction was collected for SDS-PAGE analysis. TEM-1 bound Ni-NTA beads were washed in 50 mM NaHPO4 buffer containing 50 mM imidazole 3 x 15 min, with centrifugations at 2000 RPM for 15 min to change and replenish wash buffer. Protein was eluted using 50 mM NaHPO4 buffer containing 150 mM imidazole.

3.2.3 Peptide Synthesis

All Fmoc-amino acid derivatives and HBTU were purchased from P3 Bio. Dimethylformamide (DMF), Dichloromethane (DCM), and Piperidine from Thermofisher.

Peptides were synthesized using Solid Phase Fmoc (N-(9-fluorenyl) methoxycarbonyl) Chemistry using a ResPep SL peptide synthesizer (Intavis) at a 2 nmol scale on aminated cellulose membrane. Peptides were separated from the membrane by the addition of a linker amino acid, 6-hexanoic acid. 14 residue peptides were synthesized with fixed amino acid residues at one spot, while keeping the rest of the peptide degenerate by using an equimolar mix of all amino acids except for Cysteine. Post array treatment is as follows: membrane was

washed 3 x 5 min in 20% Piperidine in DMF, followed by 3 x 2 min washes in DMF, then 3 x 2 min washes in 100% Ethanol. The array was allowed to air dry before TFA cleavage in TFA cocktail (95% TFA, 3% Tri-isopropylsilane (TIPS), and 2% dH2O) for 2 hrs at RT. Membrane was then washed 3 x 2 min in DCM, followed by 3 x 2 min in DMF, then 2 x 3 min in Ethanol. Membrane was allowed to air dry and stored at 4°C.

Peptides were synthesized using Solid Phase Fmoc (N-(9-fluorenyl) methoxycarbonyl) Chemistry using a ResPep SL peptide synthesizer (Intavis) at a 2 μmol scale using Rink-NH_2 resin. All amino acid derivates and activator were purchased from p3bio systems. To allow for quantification, peptides were synthesized with a C-terminal tryptophan separated from the peptide by a 6-aminohecanoic acid (6-ahx) linker. After synthesis, peptides were released from the resin and protecting groups were cleaved using an acidic cleavage solution (95 % trifluoroacetic acid, 3 % tri-isopropylsilane, 2 % water). Cold di-ethyl ether (-20 °C) was used to precipitate and wash the peptides of residual cleavage solution. Once dried, pellets were dissolved in 1X PBS containing 4% acetic acid. Peptides were brought up to pH 7 using 5 M NaOH and quantified by A280 and molar extinction coefficients calculated by ProtParam Expasy. 60 μM stocks of peptides were prepared in 50 mM sodium phosphate buffer.

3.2.4 OPAL binding assay

Peptide arrays were rehydrated in anhydrous ethanol, washed in dH_2O, then equilibrated in 1X Tris Buffer Saline with 0.05% Tween20 (50 mM Tris-Cl, 350

mM NaCl, 0.05% Tween20; TBST). Peptide array was blocked in 1X TBST containing 5% Non-Fat Skim Milk for 1 hr. Residual blocking buffer was washed off with 1X TBST, and recombinant His-TEM-1 was added onto the array up to a final concentration of 0.5 μM in TBST overnight at 4 ºC. Unbound protein was washed off with subsequent 1X TBST washes for 3 x 5 min at RT. The peptide array was incubated with HisProbe™-HRP Conjugate (Thermo Scientific), diluted 1:5000 in TBST, for overnight at 4 ºC. Detection was performed using enhanced luminol based chemiluminescent substrate, and images were taken on BioRad ChemiDoc XRS+ imager. Signal intensity was quantified using Protein Array Analyzer on ImageJ.

3.2.5 Motif generation using PeSA

Quantified values from ImageJ were put into a 14x19 matrix and put through Peptide Specificity Analyst (PeSA). This software allows for a motif to be generated that can be used to predict peptides based on a user-defined threshold. Normalizations were performed to the highest quantification at each residue, which allows for a weighted motif to be generated. A threshold of 2SD above the average was used to go further. This resulted in 864 peptides, which were clustered into 96 groups based off peptide characteristics such as charge, charge density, isoelectric point (pI), Instability Index, Aromaticity, Aliphatic Index, Boman Index, and Hydroph. The top peptide in each cluster was chosen to go forth for further studying.

3.2.6 Enzyme kinetics

Nitrocefin, a colorimetric β-lactam, (Calbiochem, Cat# 484400) was the substrate used for all enzymatic assays. 5 mg of substrate is dissolved in 500 μL of Dimethyl sulfoxide (DMSO), then diluted to a working concentration of 1000 ug/mL in 100 mM sodium phosphate buffer, pH 7.4. Nitrocefin hydrolysis was monitored with the use of a BioTek plate reader, reading at set time intervals at OD_{486}.

An enzyme titration was performed from 100 nM to 1 nM of TEM-1 using 13 uM of Nitrocefin. Briefly, 25 μL of 4X TEM-1 enzyme was added to 25 μL of 100 mM sodium phosphate buffer to a flat bottom 96-well plate. 100 μL of 2X the desired final concentration of nitrocefin was added to the wells and OD_{486} was measured for 10 minutes, reading every 8 secs on a BioTek plate reader using Gen5 technology. An enzyme concentration of 2.5 nM was deemed optimal for determining initial rate of reaction, and a range of 103 – 3 μM nitrocefin was tested for K_m and V_{max} determination. The initial velocity rate at the differing concentrations was determined by the slope of the reaction at the start of the enzyme assay. A velocity vs substrate graph was plotted, along with a line Weaver Burk plot using Graphpad Prism 6. K_m and V_{max} were determined by non-linear regression plotting onto the velocity vs substrate plot.

3.2.7 Peptide screen

For inhibition assays, TEM-1 and experimental peptides were used at a final concentration of 2.5 nM and 15 μM, respectively. 25 μL of 4X (10 nM) TEM-1 was

added to 25 μL of 4X (60 μM) experimental peptide and incubated with shaking at RT for 15 minutes in a flat bottom 96-well plate. No-peptide controls were run at the beginning of each day, where 25 μL of 50 mM sodium phosphate buffer, pH 7.4 was used instead of 25 μL of 4X Peptide. Once done shaking, 100 μL of 2X (35.71 μM) Nitrocefin was added to the wells and the reaction was monitored for 10 minutes with readings every 8 sec.

3.2.8 Statistical analysis

Statistical analysis was performed using an independent students t test. Mean values of TEM-1 inhibitors velocities were tested against mean no peptide TEM-1 velocities.

3.3 Results

3.3.1 TEM-1 purification

Upon induction of BL21 DE3 transformed with the plasmid pET15b-TEM-1 with IPTG, a distinct band at a MW of 31 kDa was observed. The band is prominent in the 1 mM lysate (Lane 2) found in Figure 3.4A, and not seen in the 0 mM Lysate (Lane 3). In Figure 3.4B, there is a similar and more prominent band in the purification using Ni-NTA beads, which show a selectivity for His-rich proteins. Figure 3.4B. in lane 7 shows the 50 mM imidazole wash and there is no protein of interest being washed off. Protein elutions are shown in Fig 3.4B. in lanes 8-10, and protein samples are deemed pure. Recombinant rTEM-1 in the elution is shown with a black arrow.

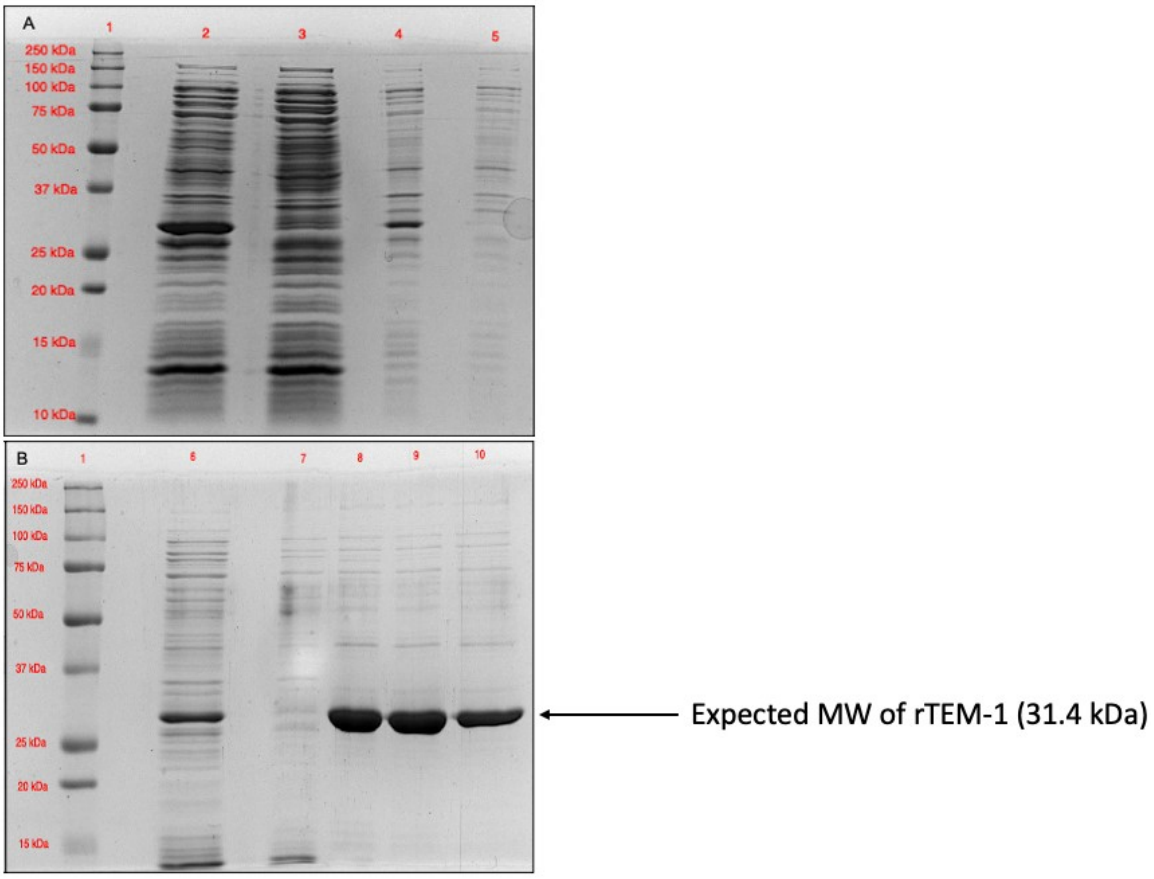

Figure 3.4. **TEM-1 expression upon TEM-1-pET15b induction.** 10% SDS-PAGE gel stained with Coomassie A. Induction for the presence of a band, Lane 2: 1 mM IPTG Lysate, Lane 3: 0 mM IPTG Lysate, Lane 4: 0 mM IPTG pellet. B. Purification of rTEM-1, lane 6: Unbound protein, Lane 7: 50 mM Imidazole wash, Lane 8-10: 150 mM Imidazole elution 1-3. Shown with the black arrow

3.3.2 Impact of amino acid residue on TEM-1 binding

Figure 3.5 shows a heat map of TEM-1 binding to the orientated peptide array library (OPAL). Using the quantification matrix from ImageJ with the use of PeSA, a motif was generated that can allow us to predict peptide sequences that bind onto TEM-1 (Figure 3.5B). A cut off 0.91 was used, and thus the motif shows us any amino acid substitution that showed 91% or greater binding per position. The motif shows an abundance of hydrophobic and polar uncharged amino acids. There is also the presence of positively charged amino acids, Arginine (R) and Lysine (K). Some positions of the motif have variability, while others are rigid in their selection. Positions 2, 5, 7, 10, 11, and 13 show a specificity for glutamine, tyrosine, leucine, threonine, isoleucine, and lysine, respectively. Position 1 shows to favour polar uncharged amino acids glutamine and tyrosine, along with positively charged arginine. Position 3 shows a preference for hydrophobic and positively charged amino acids, alanine, and arginine specifically. Position 4 acts similarly to position 1 in that positively charged amino acids and polar uncharged amino acids are tolerable. Position 6 shows a dependency for polar uncharged amino acids and hydrophobic. Position 8 shows a preference for only polar uncharged amino acids. Position 12 prefers only hydrophobic amino acids, while position 14 prefers both hydrophobic and positively charged amino acids.

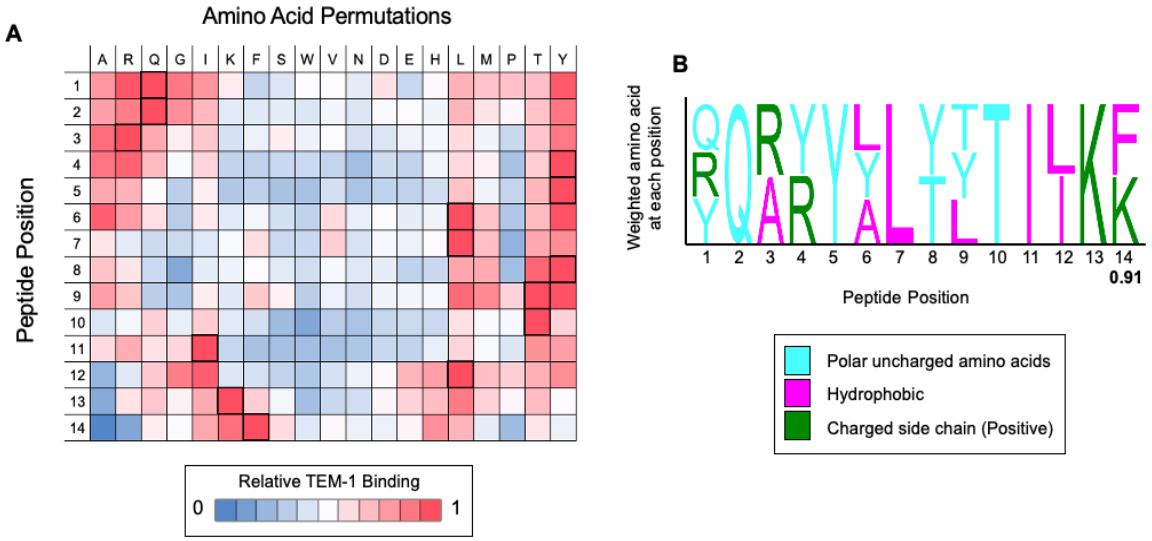

Figure 3.5. Identification of sequence motifs for TEM-1 with the use of an OPAL array. A. generated heat map for the OPAL array of 0.5 μM TEM-1. Each row was normalized to the highest quantified spot in each row, and this is shown with the boldest box. A blue hue represents little binding of TEM-1, while red represents high binding of TEM-1. B. shows the generated motif from 2σ above the mean score. This shows us the tolerability of each amino acid at each position.

3.3.3 K_m and V_{max} determination

Enzymatic conditions must be optimized for inhibition assays. Figure 3.6A shows the titration of recombinant TEM-1 from 100 nM to 1 nM using 12.9 μM of nitrocefin. The same plateau is approached over the designated time, which shows the stability of the enzyme over the assay conditions. As enzyme concentration decreases, the initial velocity of the reaction decreases as well. The enzyme produced a suitable signal over the range of time, and a concentration of 2.5 nM was deemed suitable for further enzymatic assays due to maintenance of initial linear rate. To determine the K_m and V_{max} of our recombinant TEM-1, 2.5 nM of TEM-1 was assayed against various concentrations of nitrocefin (Figure 3.6B). As nitrocefin concentration was decreased, so was the velocity of TEM-1. The velocity of each reaction is the initial slope at the beginning of the enzymatic reaction. Using substrate concentration and velocity, a direct enzymatic plot is shown in Figure 3.6C. Double reciprocal plot of velocity and substrate values are shown in Figure 3.6D. K_m and V_{max} were determined to be (35.71 $\pm$ 5.85) μM and (99.44 $\pm$ 6.95) μmol/sec, respectively, through non-linear regression analysis of the direct velocity plot using Graphpad prism 6.

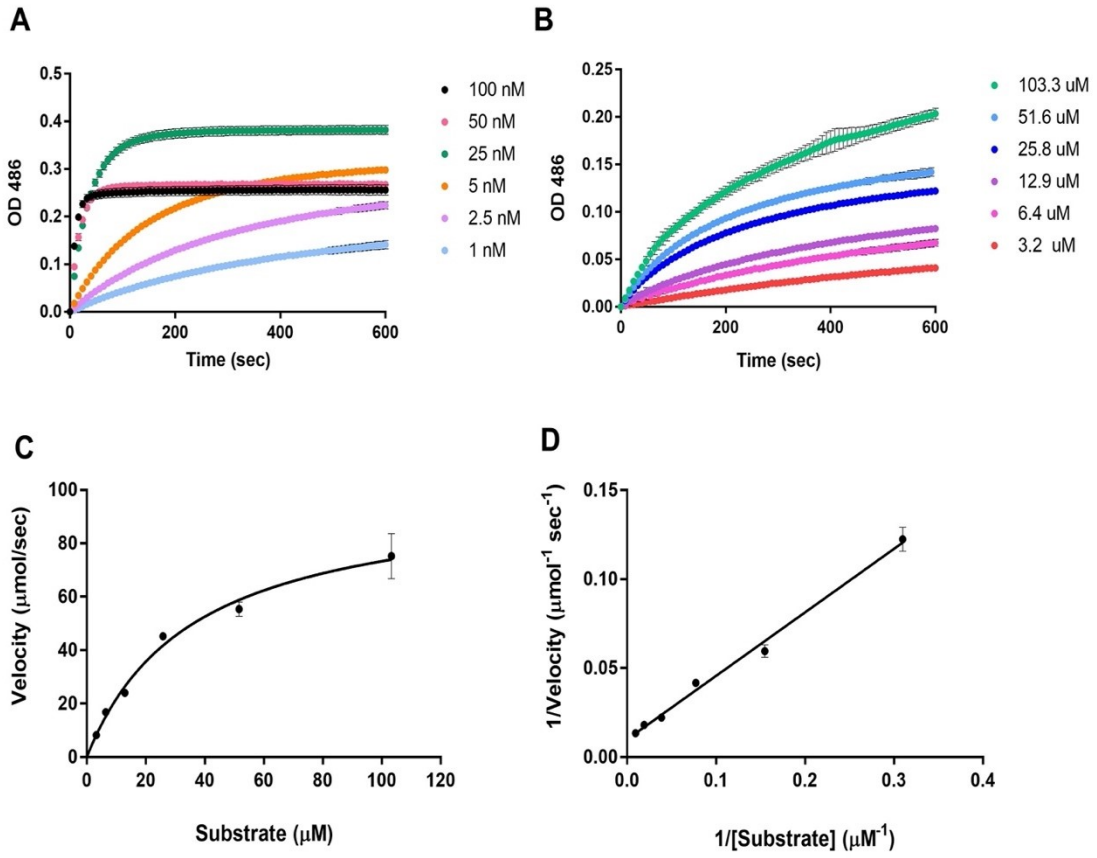

Figure 3.6. K_m and V_{max} determination for TEM-1 and Nitrocefin. A. TEM-1 titration from 100 nM to 1 nM against 12.9 μM nitrocefin. B. varying nitrocefin substrate (103 μM to 3.2 μM) against 2.5 nM TEM-1. C. direct velocity plot of initial reaction rate from panel B. D. Double reciprocal plot of 2.5 nM TEM-1 against nitrocefin (103 μM to 3.2 μM). Error bars shown as standard deviation.

3.3.4 Activity of the best performing inhibitors

Figure 3.7A represents the number of candidates that fall within the specified p-value from the 96-peptide screen for BLIs against TEM-1. This bar graph is only representative of 54 peptides out of the 96 tested. This is due to the remaining 42 peptides increased TEM-1 activity and were not used in determining peptides with inhibitory activity. Of this 54-peptide pool, 32 peptides were very significant with p-values < 0.001, 8 were significant with p-values between 0.001 and 0.01, 9 were significant with p-values between 0.01 and 0.05, and 5 peptides were found to be not significant with p-values > 0.05. Out of the 32 very significant peptides, their overall charge ranges from +5 to +1, and are due to the presence of the arginine and lysine residues. The top 5 sequences are shown Figure 3.7B. All initial velocities of the 96 peptides tested are shown in Table B1 in Appendix B.

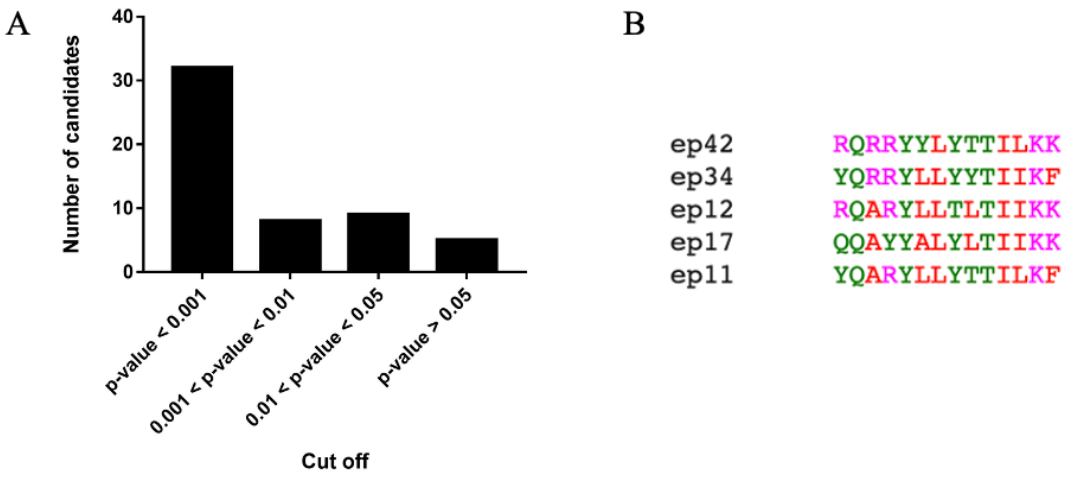

Figure 3.7. 2nd peptide generation resulted in broad range of inhibitors. A. all inhibitors that illicit a response below the control is shown with a bar graph, grouped by their p-value. B. the sequences of the top 5 inhibitors that decreased initial velocity rates of rTEM-1.

3.3.5 EP42 performs as a non-competitive inhibitor

Shown in Figure 3.8, the mechanism of the best performing peptide, EP42 was evaluated. A velocity graph was plotted by varying the concentration of substrate and keeping inhibitor concentration consistent. The inhibitor graph, shown in red, is seen to reach a lower plateau than the no inhibitor graph, shown in black. The V_{max} and K_m of the no inhibitor control is seen to be (287 $\pm$ 15.2) μmol/sec and (17.36 $\pm$ 3.002) μM respectively. The V_{max} and K_m of the EP42 treatment is (148.5 $\pm$ 8.763) μmol/sec and (12.98 $\pm$ 2.201) μM respectively.

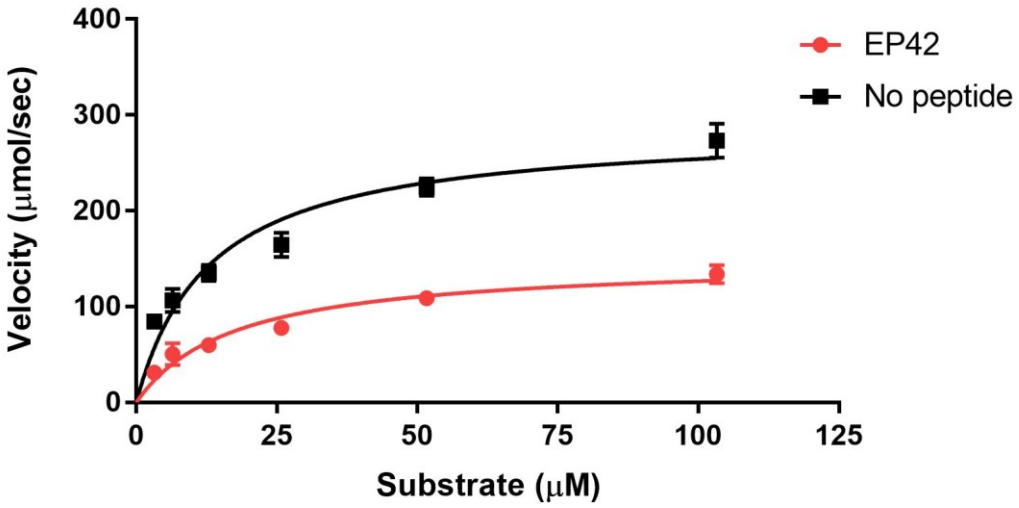

Figure 3.8. EP42 is a non-competitive inhibitor of TEM-1. Velocity curve of 15 μM EP42 while varying nitrocefin concentration (shown in red). No peptide control is shown in black. Error bars show the standard deviation.

Discussion

Development of β-lactamase inhibitors (BLIs) has been a key player in stopping resistance of β-lactamase (BLs) producing pathogens. However, overtime BLs can gain resistance and diminished therapeutic effects against the said inhibitors. The development of BLIs has been an evolving field, with many different structural inhibitors being discovered with inhibitory effects.

Here, we show the use of an orientated peptide array library to determine amino acids that are required for rTEM-1 binding. Peptides were then tested for enzymatic inhibition of rTEM-1 against nitrocefin, and their modes of action are theorized based on their structure and similarities to other peptide BLIs.

Recombinant TEM-1 (rTEM-1) protein binding was seen on various peptides with a variety of chemical characteristics. All amino acids except for cysteine were fixed for the purposes of looking at how specific amino acids can influence TEM-1 binding while the remainder of the peptide was degenerate. Degeneracy refers to the use of an equimolar mix of 19 amino acids. The heatmap that resulted from the quantification is shown in Figure 3.5A. Interestingly, there is a trend that positively charged amino acids are pertinent in binding at the start and end of the peptide, but not in the middle. Arginine is very important for binding in the first half of the peptide but not the latter half. The opposite trend is seen for lysine, where binding is optimal when lysine is found in the latter half of the peptide than the former. A peptide inhibitor of TEM-1 that was designed through both array technology and phage display libraries found arginine to be important for binding and inhibition at the C-terminus, which commemorates this discovery (Huang *et*

al., 2003). The presence of positively charged amino acid residues in the motif is not unusual, as proteins contain a negative charge on their surface at pH values above their isoelectric point (pI) (Shaw *et al*., 2001). The isoelectric point of the rTEM-1 is found to be 6.11, determined by ProtParam by Expasy. The buffer that the array is probed in is 7.4, which means rTEM-1 is overall negatively charged which can attract positively charged amino acids.

The use of SPOT synthesis allows for the rapid testing of hundreds to thousands of peptides (Huang *et al*., 2003). While this is a strong technique for the determination of peptide binding candidates, it does not show whether the peptides are inhibitors. With the use of the motif generated from the OPAL array, 96 peptides were synthesized and were tested for inhibition of rTEM-1 activity.

These peptides are different than the peptides tested on the array because they lose their degeneracy and have more defined amino acid residues. Since they originated from the same motif, they shared similar amino acid makeup, but they had variability at multiple positions.

Before peptides can be tested for inhibition, enzymatic assay conditions must be optimized to find the best linear reaction conditions. Substrate concentration was initially tested at 13 μM and an enzyme titration was performed. Low nM to pM of TEM-1 have been used in the literature for inhibition assays (Brown and Palzkill, 2010; Huang *et al*., 2003), but a wide range of concentrations were tested to assess rTEM-1 activity as other studies have used TEM-1 purified from *E. coli* isolates (Brown and Palzkill, 2010; Huang *et al*., 2003). 100 to 1 nM was tested, and 2.5 nM was determined to be best fit for the use of the enzymatic

assays going forth. Enzymatic characteristics are pertinent to understanding the modes of inhibition that can occur for enzymes, such as K_m and V_{max}. V_{max} refers to the maximum velocity that an enzyme has, and it is usually governed by the availability of substrate (Robinson, 2015). K_m, or the Michaelis constant, is the concentration of substrate that is needed for the enzyme to achieve half the V_{max}. A lower K_m values means the higher affinity that a certain compound has to a target (Robinson, 2015).

These enzymatic parameters can be estimated by measuring initial velocity of an enzyme and varying the substrate concentration. rTEM-1 was tested against 6 concentrations of nitrocefin to achieve the plots shown in figure 3.6C, D. We can either show these values as C. a direct velocity plot, or D. a double reciprocal plot. Enzymatic values can be taken by either non-linear regression of direct plot, or linear regression of the double reciprocal. There is a disadvantage to using the double reciprocal plot for estimating these values, in that it is very prone to error at low substrate concentrations (Robinson, 2015). Thus, kinetic constants were estimated by non-linear regression of Figure 3.6C, and Km and Vmax were determined to be 35.71 μM and 99.44 μmol/sec, respectively.

A broad inhibitor screen was performed against TEM-1 at a peptide concentration of 15 μM, as it is recommended initial inhibitor concentrations be tested at or below the K_m of the substrate that is used. 96 peptides were tested with only 54 peptides decreased rTEM-1 activity, and 30 of those were significant in doing so.

Modes of inhibition can be discussed and theorized based on sequence similarity to other peptide inhibitors of TEM-1. There are three main ways an inhibitor can act on an enzyme: competitive inhibition, uncompetitive inhibtion, and noncompetitive inhibition.

Competitive inhibitors are known to reduce the Km, while leaving the Vmax unaffected. The inhibitor is binding onto free enzyme and is competing for the active site with the substrate (Ramsay and Tipton, 2017), but this is not always the case. The enzyme can bind either inhibitor or substrate, but not at once. The effect of substrate concentrations is prevalent as they are competing for the active site. At high substrate concentrations, the substrate will overcome the inhibitor (Ramsay and Tipton, 2017).

Uncompetitive inhibitors reduce both the Km and Vmax and are known to bind onto the enzyme-substrate complex (Ramsay and Tipton, 2017). Saturation of inhibitor will result in the Enzyme-Substrate-Inhibitor complex to be formed, which will not no allow for product to be produced, and thus a reduction in overall enzyme performance.

Finally, non-competitive inhibitors only reduce the Vmax, leaving the Km unchanged. This is a more complex inhibitor state as it can bind to both the free enzyme and to the enzyme-substrate complex (Ramsay and Tipton, 2017).

Structural similarities between peptide-based therapeutics and β-lactam antibiotics could give insight into the mechanism of action that these peptide therapeutics could take. Other BLIs that have been characterized, such as clavulanic acid and sulbactam, are derivates of β-lactam antibiotics. These

inhibitors retain the same structure, which is the four membered lactam ring. Amino acids are strung together through peptide bonds, which is the moiety of a carbonyl-group attached to the neighbouring nitrogen.

It is known that β-lactamases have high affinity for β-lactam antibiotics, as well as for BLIs. As previously stated, BLIs that are used in most clinical settings create acyl-enzyme complexes with most BLs to stop antibiotics hydrolysis. Due to similarities in structure to the peptide bond, it can be theorized that the peptide therapeutics found from our screen might be competitive inhibitors of TEM-1 (i.e., interact directly with the active site of the enzyme).

Huang *et al*., 2003, who used both a phage display library and permutations to identify peptide inhibitors, looked at the development of peptide inhibitors against TEM-1. While they used phage display, they optimized sequences with the same SPOT synthesis as this thesis outlines. The amino acid makeup they derive and what I have outlined above complement each other nicely with the preference of arginine and glutamine in the N terminus of the peptide. Their screen resulted in a peptide sequence of RRGHYY, which is smaller than our peptide of 14 residues. They determined the type of inhibitor by the double reciprocal plots of the inhibitor at varying substrate concentrations. They found their peptide to be a competitive inhibitor, as K_m increased compared to the no peptide treatments. It was deduced that their peptide shares 50% sequence homology with the β-turn that is found in the β-lactamase inhibitory protein (BLIP) loop, which is known to have affinity to TEM-1 with Ki of 0.1-0.6 nM. Since our predict inhibitors do share some characteristics with the Huang *et al*., 2003 peptide, such as arginine and

tyrosine, it could be predicted that the inhibitors would be competitive once characterized further.

However, upon testing our top candidate EP42, we have a trend that is more representative of a non-competitive inhibitor. We see a reduction in V_{max} while little change in the K_m of TEM-1. This means that our inhibitor is reducing the activity of our enzyme by binding onto it regardless of whether there is substrate or not already bound. Compared to the peptide sequence generated from the Huang *et al*., 2003 screening, our peptide is longer in length, more hydrophobic, and more positive in charge.

Binding away from the active site (noted as an allosteric site) would deem a molecule an allosteric regulator of activity (Helmstaedt *et al*., 2001). There are known allosteric sites on TEM-1, specifically between the α11 and α12 helices of the protein (Galdadas *et al*., 2021). Since EP42 is a non-competitive inhibitor and is binding to the enzyme rather than the active site, the peptide might be binding in that helix site. Horn and Shoichet, 2004 looked at and analyzed the crystal structure of TEM-1 bound with a non-competitive inhibitor, FTA, and found that binding effected the conformation of a key catalytic residue.

An interesting avenue that could be explored is the ability for these BLIs to inhibit other Class A β-lactamases, such as SHV-1, Bla1, and CTX-M-14. They share conserved regions in their active sites (Brown and Palzkill, 2010), so there might be the application for these inhibitors to be applied as a broad BLI. The combinatory effects of our peptides with β-lactam antibiotics could be investigated, as BLIs are conventionally co-administered in clinical settings.

Chapter 4:

Final conclusions

Antimicrobial resistance is an overwhelming threat to both developed and developing countries. With mortality rates projected to increase to over 10 million by 2050, there needs to be a direct research effort towards the development of new antimicrobials, as the ones being used are showing diminishing therapeutic effects. In this regard, peptides have increased in popularity over the recent years as being a viable therapeutic for the treatment of a broad range of diseases/infections. Their versatility in their structure and range of targets is a driving force for their excellence as therapeutics (Lee *et al*., 2019).

This thesis looked at the development of peptide therapeutic to combat antimicrobial resistance. This was done by two different avenues: (1) optimization of known AMP sequences to better their antimicrobial activity, and (2) the application of an orientated peptide array library (OPAL) to determine peptide BLIs.

Optimizations of peptides to observe better activity is not a new phenomenon (Di, 2014) and has been exploited for the use of drug manufacturing. It allows for the finding of diverse peptides for specific targets that are being explored. Our results show that systematic permutations to varying amino acids show varying characteristics for antimicrobial activity. Lyamichev *et al*., 2017 looked at the stepwise evolution of peptides and increasing their binding activity against streptavidin. Their study showed that through specific permutations and insertions of new amino acids, there was an increased affinity of peptides to

streptavidin. While this study gave rise to peptides that increased affinity, some peptide permutations resulted in either no change or decreased affinity.

Amino acids permutations and directed evolution are not the only technique that can be used for identification of peptide candidates. Phage display libraries have been an emerging technique for the development of peptide therapeutics. This involves the expression of the therapeutic that is to be tested (peptide, protein, etc) on the surface of the phage and subsequent affinity steps are done to observe binding candidates to a therapeutic target (Smith and Petrenko, 1997).

With the use of amino acid permutations, we successfully increased the antimicrobial properties of UyCT3 by the mutation of several residues in the AMP sequence, resulting in UyCT3$_{I5A,\ W6Y,\ K10I,\ F13I}$. This AMP had less hemolytic activity compared to the WT AMP. It also demonstrated its ability to inhibit various clinical strains at concentrations 3-fold lower compared to the WT AMP. It was theorized that due to the amphipathic nature of the resulted peptide, it would inhibit bacterial growth by the disruption of the bacterial membrane.

By permutation of UyCT3, different point permutations were assessed but it was found that combinatory mutations illicit greater antimicrobial activity. Most studies that looked at AMP permutations, only look at single mutations or mutations of the same amino acids (Smirnova *et al*., 2004). Through generations of peptide design, combinatory mutations were able to be assessed for antimicrobial activity.

Secondly, we applied an oriented peptide array library (OPAL) to discover peptide BLIs against the β-lactamase, TEM-1. A degenerate array library was

synthesized to look at the effect of amino acid position in a 14-mer peptide had on binding to rTEM-1 enzyme. A motif is then generated from the array and can be used to create more definite peptide sequences for individual testing. From this screen, 33 peptides were effective at inhibiting rTEM-1, with a necessity for a hydrophobic and positively charged amino acids. It was also theorized that the mode of inhibition might be through interaction of the active site, as the peptide bond resembles the β-lactam bond structure of the TEM-1 substrate.

The use of a peptide array allows for the screening capabilities of hundreds to thousands of peptides, and it allows for straightforward analysis of the results. It is an efficient method in discerning which amino acids are necessary for binding onto your protein target (Huang *et al*., 2003).

Different screening approaches have been done for determining inhibitors of enzymes. Peptide arrays have been a versatile and inexpensive tool for large scale screening of biomolecule interaction events (Szymczak *et al*., 2017). Phage display libraries have also been used for the identification of enzyme inhibitors, and even a combination of these two techniques (Huang *et al*., 2003). Enzyme-linked immunosorbent assays have been used as a screening tool as well.

Through the techniques outlined in this thesis, I was able to both optimize the activity of the AMP UyCT3 through peptide evolution as well as develop peptide BLIs against the β-lactamase TEM-1. Their activity was evaluated by observing growth rates in both WT and clinical *E. coli* strains. Our promising AMP candidate from our screen did not have detrimental effects on hemolytic activity.

Translating my research towards its clinical application(s), UyCT3$_{I5A, W6Y, K10I, F13I}$ could be used in the treatment of bacterial infections, specifically urinary tract infections (UTIs) as it inhibited growth at concentration lower than UyCT3 against clinical strain, pb3. Delivery of AMPs to patient is discussed in the literature and often needs to be optimized for optimal delivery. Most peptide therapeutics are administered intravenously over orally to avoid degradation by proteases found in the oral cavity (Bruno *et al*., 2013). However, oral administration of peptide therapeutics has become more popular by the advancements of oral delivery systems, such as liposomes and nanoparticles (Bruno *et al*., 2013). I believe UyCT3$_{I5A, W6Y, K10I, F13I}$ might work through intravenous administration due to its amphipathic nature reacting with liposomes. Coating of urinary tract catheters with antimicrobial agents has also been seen to be effective against prevalence of infection as well as accumulation of biofilms (Narayana *et al*., 2019).

UyCT3$_{I5A, W6Y, K10I, F13I}$ was able to inhibit growth completely at 20 μM, which is lower than what other AMPs have been found in the literature (Wnorowska *et al*., 2019). This study had shown the efficacy of LL-37, which is a well-known AMP, against various *E. coli* UTI strains. They had found minimum inhibitory concentration (MICs) ranging from 32 – 128 μM for four separate strains. While we did not investigate MICs, 20 μM of UyCT3$_{I5A, W6Y, K10I, F13I}$ did not show any bacteria growth across the tested period. Compared to other AMPs against UTIs, our AMP inhibits better against a clinical background.

Peptide inhibitors of the β-lactamase TEM-1 were developed using an orientated peptide array library (OPAL), and the activity of peptide candidates were

tested for enzymatic inhibition. Mode of inhibition was theorized to be competitive due to both structural similarities to β-lactam antibiotics, and peptide BLIs found in the literature. Before any applications to clinical settings, the peptides would need to be furthered characterized. Peptide BLIs in the literature have been cited with their K_i values, which gives more insight into the inhibition pattern (Huang *et al*., 2003). It would also be beneficial to look at the inhibitory effects of our predicted peptides alongside β-lactam antibiotics. As for the administration of these BLIs, it would be by intravenous administration (Pandey and Cascella, 2021).

With the use of these techniques, antimicrobial agents can be developed and can be used in the fight against antimicrobial resistance. With the techniques discussed in this thesis, they can be applied to other AMPs to improve their antimicrobial activity or for the discovery of other enzymes that might dampen the efficacy of antimicrobial therapies.

Appendix A

Table A1. Peptides and growth rates for various UyCT3 derivates against *E. coli* MG1655 K-12 in MHB.

Peptide	Growth rate relative to No AMP	SEM
lLSAIWSGIKSLF	0.17656728	0.02670645
SAISFWLSIGLIK	0.40401941	0.07400773
ILSAISSGILSLIaW	0.20228315	0.04068199
lLSAIDSGIMSLFaW	0.45443418	0.11468989
lLSAAMSGIKSLVaW	0.53635804	0.12563801
lLSAAYSGIISLIaW	-0.005851	-0.0001551
lLSAISSGIISLMaW	0.21915853	0.03973375
lLSAIQSGIMSLMaW	0.98848505	0.26101353
lLSAARSGIMSLIaW	1.01382272	0.21234473
lLSAAVSGICSLIaW	1.06354991	0.23493048
lLSAAMSGICSLVaW	0.3704555	0.08763575
lLSAAESGITSLFaW	0.2999491	0.05409931
lLSAIRSGIKSLMaW	0.27930792	0.04999154
lLSAIMSGITSLIaW	0.735437	0.17964025
lLSAIDSGITSLVaW	0.84104543	0.1888168
lLSAASSGITSLIaW	0.9769414	0.23134087
lLSAIKSGITSLVaW	0.97147114	0.32109735
lLSAAYSGIISLGaW	1.09105136	0.29160737
lLSAAFSGILSLFaW	0.61249422	0.12100189
lLSAITSGITSLIaW	0.745384	0.14072738
lLSAIDSGIISLMaW	0.67663312	0.13303549
lLSAIKSGITSLFaW	0.980889	0.29315731
lLSAAASGICSLFaW	0.94334828	0.17701035
lLSAACSGITSLVaW	0.7317577	0.13671978
lLSAIVSGILSLMaW	0.38997024	0.07550994
lLSAIESGIKSLVaW	0.73851921	0.15557431
lLSAICSGIISLFaW	0.50693709	0.09564388
lLSAAWSGIKSLG	0.74738703	0.13459099
lLSAAMSGITSLMaW	0.84010813	0.18582407
lLSAATSGITSLFaW	1.0307594	0.2695005
lLSAACSGIMSLVaW	0.59630637	0.15357672
lLSAAESGIMSLIaW	0.65930676	0.18814494
lLSAIVSGILSLIaW	0.73195273	0.14174572
lLSAARSGICSLIaW	0.35908041	0.07301176
lLSAIHSGICSLGaW	0.74921964	0.21799336
lLSAAKSGIKSLVaW	0.37723017	0.10260509
lLSAAVSGIMSLGaW	0.28864249	0.06731951
lLSAIESGIISLLaW	0.67060256	0.18750702
lLSAAFSGICSLIaW	0.47560142	0.10355194
lLSAATSGIISLFaW	0.59252119	0.14953984
lLSAICSGIISLLaW	0.49604008	0.12358637
lLSAAWSGIKSLF	0.51446364	0.11777704
lLSAICSGIKSLGaW	0.21875849	0.04022622
lLSAIDSGIISLLaW	0.46745817	0.09947318
lLSAAVSGIISLFaW	0.59701075	0.14192126

lLSAAWSGIISLI	0.45626385	0.10483636
lLSAAFSGICSLlaW	0.55757703	0.13623349
lLSAIYSGICSLFaW	0.23252952	0.04658719
lLSAINSGIMSLGaW	0.48425191	0.10338417
lLSAAISGIMSLlaW	0.51881759	0.10509426
lLSAIISGIMSLLaW	-0.0026448	1.3054E-06
lLSAAESGICSLVaW	0.35605335	0.0727732
lLSAIKSGIKSLlaW	0.48763197	0.11212287
lLSAATSGICSLVaW	0.53956151	0.14786708
lLSAIHSGILSLGaW	0.56892515	0.10582294
lLSAIFSGIKSLVaW	0.53904152	0.09584655
lLSAICSGIMSLFaW	0.58632742	0.09437416
lLSAIHSGIKSLGaW	0.53956135	0.08753375
lLSAACSGIKSLMaW	0.48778832	0.09747697
lLSAIWSGITSLI	0.53436997	0.14521311
lLSAADSGITSLVaW	0.0491572	0.00759546
lLSAAQSGIKSLFaW	0.57165523	0.12702379
lLSAAWSGITSLV	0.13365736	0.0226098
lLSAAYSGIKSLlaW	0.4325072	0.08593557
lLSAAKSGILSLVaW	0.12633816	0.02163837
lLSAIRSGITSLVaW	0.1150289	0.01879331
lLSAAWSGILSLF	0.04528246	0.00688959
lLSAAYSGIMSLVaW	0.44992946	0.09303278
lLSAARSGIISLlaW	0.06728855	0.01058292
lLSAITSGIMSLFaW	0.11370357	0.0190363
lLSAAMSGITSLFaW	0.57763688	0.13987858
lLSAAGSGITSLVaW	0.79004551	0.18951809
lLSAIESGITSLMaW	0.54082437	0.12425098
lLSAAWSGITSLF	0.58264296	0.13560721
lLSAATSGIKSLVaW	0.47864067	0.09472995
lLSAARSGICSLGaW	0.50889537	0.11228253
lLSAACSGIMSLGaW	0.54014817	0.12769054
lLSAIVSGILSLFaW	0.59075015	0.13927351
lLSAAISGIMSLFaW	0.68587057	0.15343675
lLSAAMSGILSLlaW	0.62253145	0.13600415
lLSAAESGIISLFaW	0.56047544	0.1378096
lLSAIMSGIMSLMaW	0.58249141	0.13929819
lLSAISSGILSLFaW	0.56415531	0.12403913
lLSAIYSGIISLFaW	0.63147403	0.13942811
lLSAATSGICSLFaW	0.65746138	0.14551133
lLSAAPSGIKSLVaW	0.69334708	0.16590067
lLSAITSGICSLVaW	0.97183531	0.20228317
lLSAARSGIISLFaW	0.65555229	0.14840293
lLSAICSGIKSLlaW	0.70786057	0.1442522
lLSAAVSGIKSLVaW	0.6356812	0.14513688
lLSAIISGITSLVaW	0.65575858	0.14998136
lLSAIESGILSLGaW	0.64564197	0.14904532
lLSAAISGICSLMaW	0.90533583	0.1941613
lLSAAQSGIISLMaW	0.6405785	0.14645673
lLSAIDSGIKSLMaW	0.17656728	0.02670645
lLSAIKSGIISLVaW	0.40401941	0.07400773
lLSAAVSGITSLVaW	0.20228315	0.04068199
lLSAATSGITSLGaW	0.64887567	0.07885822
lLSAAISGIMSLMaW	0.65412203	0.11080245
lLSAIYSGICSLMaW	0.59677663	0.04349064
lLSAILSGITSLlaW	0.5434635	0.07971955
lLSAICSGIMSLlaW	0.49337245	0.02978773
lLSAAKSGICSLVaW	0.44939128	0.05733173

Table A2. Peptides and growth rates for various Indolicidin derivates against *E. coli* MG1655 K-12 in MHB.

Peptide	Growth rate	SEM
ILPWKWPWWPWRR	0.12490985	0.01989391
ILPWAWPWWPWRR	0.00123058	0.00058643
ILPWCWPWWPWRR	0.00123986	0.00032453
ILPWDWPWWPWRR	0.00101299	0.00030005
ILPWEWPWWPWRR	0.64707679	0.15688291
ILPWFWPWWPWRR	0.3640633	0.07975484
ILPWGWPWWPWRR	0.55575277	0.13937779
ILPWHWPWWPWRR	1.02850762	0.25749153
ILPWIWPWWPWRR	0.64476826	0.13560645
ILPWLWPWWPWRR	0.00030671	0.00127628
ILPWMWPWWPWRR	0.14683178	0.02388204
ILPWNWPWWPWRR	0.0832804	0.01614329
ILPWPWPWWPWRR	0.12831806	0.01863232
ILPWQWPWWPWRR	0.18937901	0.02941555
ILPWRWPWWPWRR	0.59493179	0.11711517
ILPWSWPWWPWRR	0.2291982	0.04169555
ILPWTWPWWPWRR	0.51719785	0.09937755
ILPWVWPWWPWRR	0.15746893	0.02693132
ILPWWWPWWPWRR	0.42638118	0.09604778
ILPWYWPWWPWRR	0.32554978	0.07087217

Appendix B

Table B1. Peptides and initial velocities for 2nd generation OPAL peptides against rTEM-1.

Peptide	Velocity relative to no Peptide	SEM
RQRYYALYTTIIKKaW	0.37090909	0.14454757
YQRYYALTLTILKFaW	0.26008798	0.05220403
RQRRYALYTTIIKKaW	0.36730463	0.05600662
YQRYYYLYTTILKKaW	0.67954545	0.07931745
RQARYYLYTTILKFaW	0.26548688	0.0609449
YQRRYALTLTILKFaW	1.48272727	0.10273854
RQARYLLTTTIIKKaW	3.57272727	0.05673259
YQRYYYLTLTIIKKaW	2.94	0.05355359
RQRRYALTTTIIKKaW	2.35066155	0.05213858
QQARYLLTTTIIKKaW	0.35446009	0.16577652
YQARYLLYTTILKFaW	0.08652943	0.09192781
RQARYLLTLTIIKKaW	0.06717226	0.07294971
YQARYYLTTTIIKKaW	0.49514867	0.09177648
YQAYYALTLTILKFaW	0.42018779	0.09115447
RQRRYYLYTTILKFaW	2.36244131	0.05224551
YQRRYLLTLTILKKaW	0.55758998	0.08466533
QQAYYALYLTIIKKaW	0.08154285	0.07165725
QQAYYLLYTTILKFaW	1.43192488	0.13457708
QQRRYALYTTIIKKaW	2.16601767	0.05327628
RQRRYALTLTIIKKaW	2.61525361	0.05744627
YQRYYALTTTILKFaW	1.40099587	0.08437445
RQAYYLLTLTIIKKaW	0.56807512	0.12586754
RQAYYYLYTTILKFaW	0.72101295	0.13962542
RQARYLLTLTIIKFaW	0.92331768	0.07379984
YQRRYYLYTTIIKKaW	3.89201878	0.05394369
YQARYALTTTILKFaW	1.32379921	0.07038491
RQRRYLLYTTILKFaW	2.68779343	0.06971445
YQAYYYLYTTILKFaW	0.65070423	0.10664435
QQARYALYTTILKKaW	2.81993499	0.05023073
QQAYYALYTTILKKaW	3.23928013	0.04480926
QQARYALTLTIIKFaW	1.10328638	0.07878363
QQRRYALYLTIIKKaW	0.52816901	0.11424694
YQRYYALYTTIIKFaW	0.2444926	0.07329894
YQRRYLLYYTIIKFaW	0.05525637	0.31834465
QQAYYYLYTTIIKKaW	0.52243007	0.06814752
YQRRYYLTTTILKKaW	1.31665673	0.04895648
RQARYALYTTILKKaW	0.24413146	0.0736572
RQRRYALYTTILKFaW	0.20515009	0.05821824
YQRYYALYTTIIKKaW	1.99777613	0.04769597
QQRRYALTLTIIKFaW	0.80745483	0.15110134
QQARYLLYYTIIKKaW	1.70075567	0.07500145
RQRRYYLYTTILKKaW	0.00242778	0.29175238
QQAYYLLYLTIIKFaW	0.19106938	0.16838541
QQRRYALYTTIIKFaW	2.30309137	0.05844964
YQRYYALTLTILKKaW	5.76221662	0.0920266
YQARYALTLTILKKaW	4.37822127	0.07344706
RQARYYLTLTIIKKaW	2.19088619	0.05497691
YQRYYALTTTILKKaW	0.52063334	0.08316678
RQRYYLLYTTILKKaW	0.65743073	0.04888022
RQARYYLYLTILKKaW	0.64677028	0.06310914
YQARYLLTTTIIKKaW	2.1546212	0.05260425
YQRRYALYTTIIKFaW	1.48733146	0.05719385
YQRYYALYLTILKKaW	0.32391546	0.1063567
RQARYALYTTILKFaW	1.34069155	0.06665201

QQARYALTLTIIKKaW	2.08936253	0.06074495
QQRRYYLYTTILKFaW	0.45907946	0.13749925
QQRRYALYYTIIKFaW	0.26428987	0.11506154
YQAYYLLYTTILKFaW	0.65155332	0.0921984
YQRYYYLYTTILKFaW	0.60375896	0.12741066
YQAYYALYTTILKFaW	0.41561713	0.14615908
RQARYLLTTTILKFaW	0.93368998	0.06758854
QQARYLLTTTILKFaW	0.40528967	0.08813935
RQRYYYLYTTILKFaW	0.8070585	0.078821
YQAYYYLYTTIIKKaW	1.70252652	0.08656958
YQRYYLLTLTILKKaW	0.51307886	0.06765399
YQRYYLLTLTIIKFaW	0.40426274	0.05747717
RQARYYLTLTIIKFaW	2.12846348	0.08467305
QQRYYALYYTIIKKaW	6.03856194	0.08974098
QQAYYLLTTTILKFaW	1.73535784	0.05910958
YQARYLLTTTILKFaW	5.30982368	0.09769617
RQRYYLLTLTILKFaW	0.48857339	0.07925227
YQRRYYLYTTILKFaW	1.11777727	0.08103545
QQRYYLLYTTILKKaW	2.48903137	0.05941546
YQRRYYLYLTIIKKaW	2.51083123	0.07848861
QQARYALYLTILKKaW	0.3198464	0.0818922
RQARYALTLTILKKaW	1.12594458	0.06587399
QQRRYALTTTIIKKaW	0.43712459	0.06323631
RQARYLLYLTILKKaW	0.4364247	0.07487984
YQARYLLTLTILKKaW	0.87327685	0.06377981
RQRRYYLTLTIIKKaW	1.7072449	0.05948442
RQAYYALYTTIIKFaW	1.46572017	0.07644662
YQARYLLYLTILKKaW	1.23425693	0.12260095
YQRYYYLTLTILKFaW	1.33299748	0.09756668
RQRYYALYLTILKFaW	0.98740554	0.11064817
YQRRYLLYTTILKFaW	0.72153271	0.07043428
QQARYALYYTIIKKaW	0.58560415	0.08280931
RQRYYLLYTTILKFaW	0.77881078	0.0705636
QQRRYLLYYTIIKKaW	1.95514846	0.0573945
RQARYALTLTILKFaW	2.75314861	0.08400877
RQAYYLLTLTIIKFaW	1.63425693	0.07607543
QQARYYLTLTIIKKaW	2.49533036	0.06297075
RQRRYLLYLTILKFaW	0.67619031	0.07395144
YQAYYLLYLTIIKFaW	4.28211587	0.08151186
RQRRYLLTTTILKFaW	0.56506149	0.06464322
RQRRYLLTLTIIKKaW	0.77413938	0.09434034
RQRRYLLYYTILKFaW	0.20631661	0.07430733

References

Ahmed S, Mathews AS, Byeon N, Lavasanifar A, Kaur K. 2010. Peptide arrays for screening cancer specific peptides. Analytical Chemistry **82**:7533–7541.

Alaybeyoglu B, Uluocak BG, Akbulut BS, Ozkirimli E. 2017. The effect of a beta-lactamase inhibitor peptide on bacterial membrane structure and integrity: A comparative study. Journal of Peptide Science **23**:374–383.

Almaaytah A, Albalas Q. 2014. Scorpion venom peptides with no disulfide bridges: A Review. Peptides **51**:35–45.

Aminov RI. 2010. A brief history of the antibiotic era: Lessons learned and challenges for the future. Frontiers in Microbiology **1**.

Bagel S, Hüllen Volker, Wiedemann B, Heisig P. 1999. Impact of gyra and parc mutations on quinolone resistance, doubling time, and supercoiling degree of escherichia coli. Antimicrobial Agents and Chemotherapy **43**:868–875.

Bahar A, Ren D. 2013. Antimicrobial peptides. Pharmaceuticals **6**:1543–1575.

Bartlett JG, Gilbert DN, Spellberg B. 2013. Seven ways to preserve the miracle of antibiotics. Clinical Infectious Diseases **56**:1445–1450.

Basra P, Alsaadi A, Bernal-Astrain G, O'Sullivan ML, Hazlett B, Clarke LM, Schoenrock A, Pitre S, Wong A. 2018. Fitness tradeoffs of antibiotic

resistance in extraintestinal pathogenic escherichia coli. Genome Biology and Evolution **10**:667–679.

Beadle BM, Nicholas RA, Shoichet BK. 2001. Interaction energies between β-lactam antibiotics and E. coli penicillin-binding protein 5 by reversible thermal denaturation. Protein Science **10**:1254–1259.

Bradford PA. 2001. Extended-spectrum β-lactamases in the 21st century: Characterization, epidemiology, and detection of this important resistance threat. Clinical Microbiology Reviews **14**:933–951.

Brolund A. 2014. Overview of ESBL-producing *enterobacteriaceae* from a nordic perspective. Infection Ecology & Epidemiology **4**:24555.

Brown NG, Palzkill T. 2010. Identification and characterization of β-lactamase inhibitor protein-II (BLIP-II) interactions with β-lactamases using phage display. Protein Engineering, Design and Selection **23**:469–478.

Browne K, Chakraborty S, Chen R, Willcox MDP, Black DSC, Walsh WR, Kumar N. 2020. A new era of antibiotics: The clinical potential of antimicrobial peptides. International Journal of Molecular Sciences **21**:7047.

Bruno BJ, Miller GD, Lim CS. 2013. Basics and recent advances in peptide and protein drug delivery. Therapeutic Delivery **4**:1443–1467.

Burmeister AR. 2015. Horizontal gene transfer. Evolution, Medicine, and Public Health **2015**:193–194.

Bush K, Bradford PA. 2016. B-lactams and β-lactamase inhibitors: An overview. Cold Spring Harbor Perspectives in Medicine **6**.

Canada PHAof. 2020. Government of Canada. Canadaca. / Gouvernement du Canada.

Carcione D, Siracusa C, Sulejmani A, Leoni V, Intra J. 2021. Old and new beta-lactamase inhibitors: Molecular structure, mechanism of action, and clinical use. Antibiotics **10**:995.

Chang Q, Wang W, Regev-Yochay G, Lipsitch M, Hanage WP. 2014. Antibiotics in agriculture and the risk to human health: How worried should we be? Evolutionary Applications **8**:240–247.

Chen CH, Lu TK. 2020. Development and challenges of antimicrobial peptides for therapeutic applications. Antibiotics **9**:24.

Cho H, Uehara T, Bernhardt TG. 2014. Beta-lactam antibiotics induce a lethal malfunctioning of the bacterial cell wall synthesis machinery. Cell **159**:1300–1311.

Chopra A, Willmore W, Biggar K. 2022. Insights into a cancer-target demethylase: Substrate prediction through systematic specificity analysis for KDM3A. Biomolecules **12**:641.

Chrom C, Renn L, Caputo G. 2019. Characterization and antimicrobial activity of amphiphilic peptide AP3 and derivative sequences. Antibiotics **8**:20.

Coates ARM, Halls G, Hu Y. 2011. Novel classes of antibiotics or more of the same? British Journal of Pharmacology **163**:184–194.

Cutrona KJ, Kaufman BA, Figueroa DM, Elmore DE. 2015. Role of arginine and lysine in the antimicrobial mechanism of histone-derived antimicrobial peptides. FEBS Letters **589**:3915–3920.

Dadgostar P. 2019. Antimicrobial resistance: Implications and costs. Infection and Drug Resistance **Volume 12**:3903–3910.

Davies J. 2006. Where have all the antibiotics gone? Canadian Journal of Infectious Diseases and Medical Microbiology **17**:287–290.

Di L. 2014. Strategic approaches to optimizing peptide ADME properties. The AAPS Journal **17**:134–143.

Dijksteel GS, Ulrich MM, Middelkoop E, Boekema BK. 2021. Review: Lessons learned from clinical trials using antimicrobial peptides (AMPS). Frontiers in Microbiology **12**.

Drawz SM, Bonomo RA. 2010. Three decades of β-lactamase inhibitors. Clinical Microbiology Reviews **23**:160–201.

Dutescu IA, Hillier SA. 2021. Encouraging the development of new antibiotics: Are financial incentives the right way forward? A systematic review and case study. Infection and Drug Resistance **Volume 14**:415–434.

El-Sayed Ahmed MA, Zhong L-L, Shen C, Yang Y, Doi Y, Tian G-B. 2020. Colistin and its role in the era of antibiotic resistance: An extended review (2000–2019). Emerging Microbes & Infections **9**:868–885.

Giacomini E, Perrone V, Alessandrini D, Paoli D, Nappi C, Degli Esposti L. 2021. Evidence of antibiotic resistance from population-based studies: A narrative review. Infection and Drug Resistance **Volume 14**:849–858.

Golkar Z, Bagasra O, Pace DG. 2014. Bacteriophage therapy: A potential solution for the antibiotic resistance crisis. The Journal of Infection in Developing Countries **8**:129–136.

Gould IM, Bal AM. 2013. New antibiotic agents in the pipeline and how they can help overcome microbial resistance. Virulence **4**:185–191.

Greco I, Molchanova N, Holmedal E, Jenssen H, Hummel BD, Watts JL, Håkansson J, Hansen PR, Svenson J. 2020. Correlation between hemolytic activity, cytotoxicity, and systemic in vivo toxicity of synthetic antimicrobial peptides. Scientific Reports **10**.

Grigorenko VG, Andreeva IP, Rubtsova MY, Deygen IM, Antipin RL, Majouga AG, Egorov AM, Beshnova DA, Kallio J, Hackenberg C, Lamzin VS. 2017. Novel non-β-lactam inhibitor of β-lactamase TEM-171 based on Acylated Phenoxyaniline. Biochimie **132**:45–53.

Hammers CM, Stanley JR. 2014. Antibody phage display: Technique and applications. Journal of Investigative Dermatology **134**:1–5.

Hart BL. 2011. Behavioural defences in animals against pathogens and parasites: Parallels with the Pillars of medicine in humans. Philosophical Transactions of the Royal Society B: Biological Sciences **366**:3406–3417.

Hasan CM, Dutta D, Nguyen AN. 2021. Revisiting antibiotic resistance: Mechanistic foundations to evolutionary outlook. Antibiotics **11**:40.

Hoekstra M, Biggar KK. 2021. Identification of in vitro JMJD lysine demethylase candidate substrates via systematic determination of substrate preference. Analytical Biochemistry **633**:114429.

Hsu C-H. 2005. Structural and DNA-binding studies on the bovine antimicrobial peptide, indolicidin: Evidence for multiple conformations involved in binding to membranes and DNA. Nucleic Acids Research **33**:4053–4064.

Huan Y, Kong Q, Mou H, Yi H. 2020. Antimicrobial peptides: Classification, design, application, and research progress in multiple fields. Frontiers in Microbiology **11**.

Huang W, Beharry Z, Zhang Z, Palzkill T. 2003. A broad-spectrum peptide inhibitor of -lactamase identified using phage display and peptide arrays. Protein Engineering Design and Selection **16**:853–860.

Iskandar K, Murugaiyan J, Hammoudi Halat D, Hage SE, Chibabhai V, Adukkadukkam S, Roques C, Molinier L, Salameh P, Van Dongen M. 2022. Antibiotic discovery and resistance: The Chase and the race. Antibiotics **11**:182.

Iwu CD, Korsten L, Okoh AI. 2020. The incidence of antibiotic resistance within and beyond the agricultural ecosystem: A concern for public health. MicrobiologyOpen **9**.

Jaktaji RP, Mohiti E. 2010. Study of Mutations in the DNA gyrase gyrA Gene of Escherichia coli. Iranian Journal of Pharmaceutical Research **9**:43–48.

Kapoor G, Saigal S, Elongavan A. 2017. Action and resistance mechanisms of antibiotics: A guide for clinicians. Journal of Anaesthesiology Clinical Pharmacology **33**:300.

King DT, Sobhanifar S, Strynadka NC. 2017. The mechanisms of resistance to β-lactam antibiotics. Handbook of Antimicrobial Resistance 177–201.

Koch P, Schmitt S, Heynisch A, Gumpinger A, Wüthrich I, Gysin M, Shcherbakov D, Hobbie SN, Panke S, Held M. 2022. Optimization of the antimicrobial peptide bac7 by deep mutational scanning. BMC Biology **20**.

Kumar N, Sood D, Tomar R, Chandra R. 2019. Antimicrobial peptide designing and optimization employing large-scale flexibility analysis of protein-peptide fragments. ACS Omega **4**:21370–21380.

Langenegger N, Nentwig W, Kuhn-Nentwig L. 2019. Spider Venom: Components, modes of action, and novel strategies in transcriptomic and Proteomic analyses. Toxins **11**:611.

Lee AC-L, Harris JL, Khanna KK, Hong J-H. 2019. A comprehensive review on current advances in peptide drug development and Design. International Journal of Molecular Sciences **20**:2383.

Lewis K. 2020. The Science of Antibiotic discovery. Cell **181**:29–45.

Llor C, Bjerrum L. 2014. Antimicrobial resistance: Risk associated with antibiotic overuse and initiatives to reduce the problem. Therapeutic Advances in Drug Safety **5**:229–241.

Luna-Ramírez K, Quintero-Hernández V, Vargas-Jaimes L, Batista CVF, Winkel KD, Possani LD. 2013. Characterization of the Venom from the australian scorpion urodacus yaschenkoi: Molecular mass analysis of components, cdna sequences and peptides with antimicrobial activity. Toxicon **63**:44–54.

Luyt C-E, Bréchot N, Trouillet J-L, Chastre J. 2014. Antibiotic stewardship in the Intensive Care Unit. Critical Care **18**.

Magdeldin S, Zhang Y, Xu B, Yoshida Y, Yamamoto T. 2012. Two-dimensional polyacrylamide gel electrophoresis - A practical perspective. Gel Electrophoresis - Principles and Basics.

Mahlapuu M, Håkansson J, Ringstad L, Björn C. 2016. Antimicrobial peptides: An emerging category of Therapeutic Agents. Frontiers in Cellular and Infection Microbiology **6**.

Marchand C, Krajewski K, Lee H-F, Antony S, Johnson AA, Amin R, Roller P, Kvaratskhelia M, Pommier Y. 2006. Covalent binding of the natural antimicrobial peptide indolicidin to DNA Abasic sites. Nucleic Acids Research **34**:5157–5165.

Massova I, Mobashery S. 1998. Kinship and diversification of bacterial penicillin-binding proteins and β-lactamases. Antimicrobial Agents and Chemotherapy **42**:1–17.

McCubbin KD, Anholt RM, de Jong E, Ida JA, Nóbrega DB, Kastelic JP, Conly JM, Götte M, McAllister TA, Orsel K, Lewis I, Jackson L, Plastow G, Wieden H-J, McCoy K, Leslie M, Robinson JL, Hardcastle L, Hollis A, Ashbolt NJ, Checkley S, Tyrrell GJ, Buret AG, Rennert-May E, Goddard E, Otto SJ, Barkema HW. 2021. Knowledge gaps in the understanding of antimicrobial resistance in Canada. Frontiers in Public Health **9**.

MEDEIROS ANTONEA. 1984. B-lactamases. British Medical Bulletin **40**:18–27.

Michael CA, Dominey-Howes D, Labbate M. 2014. The antimicrobial resistance crisis: Causes, consequences, and management. Frontiers in Public Health **2**.

Milani RV, Wilt JK, Entwisle J, Hand J, Cazabon P, Bohan JG. 2019. Reducing inappropriate outpatient antibiotic prescribing: Normative comparison using unblinded provider reports. BMJ Open Quality **8**.

Mishra B, Lakshmaiah Narayana J, Lushnikova T, Zhang Y, Golla RM, Zarena D, Wang G. 2020. Sequence permutation generates peptides with different antimicrobial and antibiofilm activities. Pharmaceuticals **13**:271.

Munita JM, Arias CA. 2016. Mechanisms of antibiotic resistance. Microbiology Spectrum **4**.

Nan YH, Park KH, Park Y, Jeon YJ, Kim Y, Park I-S, Hahm K-S, Shin SY. 2009. Investigating the effects of positive charge and hydrophobicity on the cell selectivity, mechanism of action and anti-inflammatory activity of a trp-rich antimicrobial peptide indolicidin. FEMS Microbiology Letters **292**:134–140.

Norouzy A, Assaf KI, Zhang S, Jacob MH, Nau WM. 2014. Coulomb repulsion in short polypeptides. The Journal of Physical Chemistry B **119**:33–43.

Narayana JL, Mishra B, Lushnikova T, Golla RM, Wang G. Modulation of antimicrobial potency of human cathelicidin peptides against ESKAPE pathogens and in vivo efficacy in a murine catheter-associated biofilm model. Biochimica et Biophysica Acta. **9**:1592 - 1602

Nature. 2013. The antibiotic alarm. Nature **495**:141–141.

Nothias L-F, Knight R, Dorrestein PC. 2016. Antibiotic discovery is a walk in the park. Proceedings of the National Academy of Sciences **113**:14477–14479.

O'Farrell PH. 1975. High resolution two-dimensional electrophoresis of proteins. Journal of Biological Chemistry. **250**(10). 4007-21.

Olshina MA, Sharon M. 2016. Mass Spectroscopy: A Technique of Many Faces. Quarterly Reviews of Biophysics. **49**(18).

Pandey N, Cascella M. 2021. Beta Lactam Antibiotics. Stats Pearl.

Penicillin's finder assays its future; Sir Alexander Fleming says Improved Dosage Method Is Needed To Extend Use Other Scientists Praised Self-Medication Decried. The New York Times. 1945.

Ramirez J, Guarner F, Bustos Fernandez L, Maruy A, Sdepanian VL, Cohen H. 2020. Antibiotics as major disruptors of gut microbiota. Frontiers in Cellular and Infection Microbiology **10**.

Ramsay R, Tipton K. 2017. Assessment of Enzyme Inhibition: A review with examples from the development of monoamine oxidase and cholinesterase inhibitory drugs. Molecules **22**:1192.

Read AF, Woods RJ. 2014. Antibiotic resistance management. Evolution, Medicine, and Public Health **2014**:147–147.

Recio C, Maione F, Iqbal AJ, Mascolo N, De Feo V. 2017. The potential therapeutic application of peptides and peptidomimetics in cardiovascular disease. Frontiers in Pharmacology **7**.

Reineke U, Volkmer-Engert R, Schneider-Mergener J. 2001. Applications of peptide arrays prepared by the spot-technology. Current Opinion in Biotechnology **12**:59–64.

Reygaert W. 2018. An overview of the antimicrobial resistance mechanisms of bacteria. AIMS Microbiology **4**:482–501.

Robinson PK. 2015. Enzymes: Principles and biotechnological applications. Essays in Biochemistry **59**:1–41.

Rodriguez M, Li SS-C, Harper JW, Songyang Z. 2004. An Oriented Peptide Array Library (OPAL) strategy to study protein-protein interactions. Journal of Biological Chemistry **279**:8802–8807.

Rosenblatt-Farrell N. 2009. The landscape of antibiotic resistance. Environmental Health Perspectives **117**.

Rudgers GW, Huang W, Palzkill T. 2001. Binding properties of a peptide derived from β-lactamase inhibitory protein. Antimicrobial Agents and Chemotherapy **45**:3279–3286.

Shaw KL, Grimsley GR, Yakovlev GI, Makarov AA, Pace CN. 2001. The effect of net charge on the solubility, activity, and stability of Ribonuclease SA. Protein Science **10**:1206–1215.

Shreiner AB, Kao JY, Young VB. 2015. The gut microbiome in health and in disease. Current Opinion in Gastroenterology **31**:69–75.

Simpkin VL, Renwick MJ, Kelly R, Mossialos E. 2017. Incentivising innovation in antibiotic drug discovery and development: Progress, challenges, and next steps. The Journal of Antibiotics **70**:1087–1096.

Smirnova MP, Afonin VG, Shpen' VM, Tyagotin YV, Kolodkin NI. 2004. Structure–function relationship between analogues of the antibacterial peptide indolicidin. I. Synthesis and biological activity of analogues with increased amphipathicity and elevated net positive charge of the molecule. Russian Journal of Bioorganic Chemistry **30**:409–416.

Strempel N, Strehmel J, Overhage J. 2014. Potential application of antimicrobial peptides in the treatment of bacterial biofilm infections. Current Pharmaceutical Design **21**:67–84.

Subbalakshmi C, Sitaram N. 2006. Mechanism of antimicrobial action of indolicidin. FEMS Microbiology Letters **160**:91–96.

Szymczak LC, Kuo H-Y, Mrksich M. 2017. Peptide arrays: Development and application. Analytical Chemistry **90**:266–282.

Tipper DJ, Strominger JL. 1965. Mechanism of action of Penicillins: A proposal based on their structural similarity to acyl-D-alanyl-D-alanine. Proceedings of the National Academy of Sciences **54**:1133–1141.

Tooke CL, Hinchliffe P, Bragginton EC, Colenso CK, Hirvonen VHA, Takebayashi Y, Spencer J. 2019. B-lactamases and β-lactamase inhibitors in the 21st Century. Journal of Molecular Biology **431**:3472–3500.

Topcu E, Biggar KK. 2019. Pesa: A software tool for peptide specificity analysis. Computational Biology and Chemistry **83**:107145.

Uddin SJ, Shilpi JA, Nahar L, Sarker SD, Göransson U. 2021. Editorial: Natural antimicrobial peptides: Hope for new antibiotic lead molecules. Frontiers in Pharmacology **12**.

Vagner J, Qu H, Hruby VJ. 2008. Peptidomimetics, a synthetic tool of drug discovery. Current Opinion in Chemical Biology **12**:292–296.

Vakulenko S, Golemi D. 2002. Mutant tem β-lactamase producing resistance to ceftazidime, Ampicillins, and β-lactamase inhibitors. Antimicrobial Agents and Chemotherapy **46**:646–653.

Van Gerwen J. 2022. Ministry of Agriculture, Food and Rural Affairs. Antimicrobial Resistance in Agriculture. Ministry of Agriculture, Food, and Rural Affairs.

Ventola CL. The antibiotic resistance crisis: Part 1: Causes and threats. P & T: a peer-reviewed journal for formulary management. U.S. National Library of Medicine.

Vergis J, Malik SS, Pathak R, Kumar M, Ramanjaneya S, Kurkure NV, Barbuddhe SB, Rawool DB. 2019. Antimicrobial efficacy of indolicidin against multi-drug resistant enteroaggregative escherichia coli in a galleria mellonella model. Frontiers in Microbiology **10**.

Viswanathan VK. 2014. Off-label abuse of antibiotics by bacteria. Gut Microbes **5**:3–4.

Wang L, Wang N, Zhang W, Cheng X, Yan Z, Shao G, Wang X, Wang R, Fu C. 2022. Therapeutic peptides: Current applications and Future Directions. Signal Transduction and Targeted Therapy **7**.

Wimley WC, Hristova K. 2011. Antimicrobial peptides: Successes, challenges, and Unanswered Questions. The Journal of Membrane Biology **239**:27–34.

Wnorowska U, Piktel E, Durnas B, Fiedoruk K, Savage PB, Bucki R. 2019. Use of ceragenins as a potential treatment for urinary tract infections. BMC Infectious Diseases **19**. 369

Wright GD. 2010. Antibiotic resistance in the environment: A link to the clinic? Current Opinion in Microbiology **13**:589–594.

Wright PM, Seiple IB, Myers AG. 2014. Cheminform abstract: The evolving role of chemical synthesis in antibacterial drug discovery. ChemInform **45**.